SC

PETROLOGY OF THE GRACEFIELD PLUTON

by

Marcel Elzear Durocher

A thesis submitted to the School of Graduate Studies in partial fulfillement of the requirements for the degree of M.Sc. in Geology

UNIVERSITY OF OTTAWA
OTTAWA, CANADA, 1977

ABSTRACT

The Gracefield pluton is composed of two distinct syenite intrusions; both of which appear to have been intruded late in the Grenville tectonic and metamorphic history. They both exhibit a well developed concentric mineralogical zoning. They have shonkinitic cores which grade laterally into alkali syenite. The larger (earlier) intrusive is locally transitional to nepheline syenite along the south margin.

The temperature of mineral equilibration of the nepheline-bearing syenite was determined to be 730°C. The temperature of the magma at the time of intrusion was somewhat higher. If the oxygen fugacity during the crystallization history of the early intrusive was close to that of the QFM buffer, the fugacity of water was between 302 and 1950 bars. The silica activity in the magma was low during crystallization.

The two intrusives are mineralogically, chemically, and texturally similar. They also appear to have had similar crystallization histories. It is highly probable that the temperature of intrusion, oxygen and water fugacities, and silica activity in the later intrusive, were in the same range as those in the early intrusive.

The mineralogical zoning in the intrusives is due to the operation of convection cells during the early parts of their crystallization histories.

Shortly after emplacement of a largely liquid magma, salite, apatite, and minor amounts of magnetite and ilmenite started crystallizing along the walls of the magma chamber. These crystals were then concentrated in the lower part of the magma chamber by slow moving convection cells. This resulted in an alkalic magma in the upper part of the chamber, and a crystal mush in the lower part. After convection ceased, crystallization of the feldspars, barkevikite, biotite, most of the magnetite, and nepheline and calcite commenced in the larger intrusive.

TABLE OF CONTENTS

page

CHAPTER III

page

LIST OF TABLES

page

LIST OF FIGURES

page

page

LIST OF PLATES

page

CHAPTER I

INTRODUCTION

Location and physiography of the study area

The study area lies approximately 60 miles northwest of Ottawa, and 4 miles north of Gracefield, Quebec (Figure 1) and covers approximately 8 square miles. The area is included in the following 1/50,000 N.T.S. sheets: 31K/1E and 31J/4W . It has been glaciated and has low to moderate relief (450 feet). The topography, reflects to a considerable degree, the character of the underlying bedrock. Generally the syenitic rocks stand out above the surrounding marbles and gneisses, and are better exposed. However, in the northern part of the study area, there are numerous swamps, and the syenitic rocks are poorly exposed.

Purpose of the investigation

The object of this work is to study the petrology of the syenite pluton in this area in order to determine:

1) its position in the Grenville metamorphic and tectonic history.
2) whether the syenite pluton in question is a single differentiated intrusive or a composite intrusion.
3) the crystallization history of these rocks.

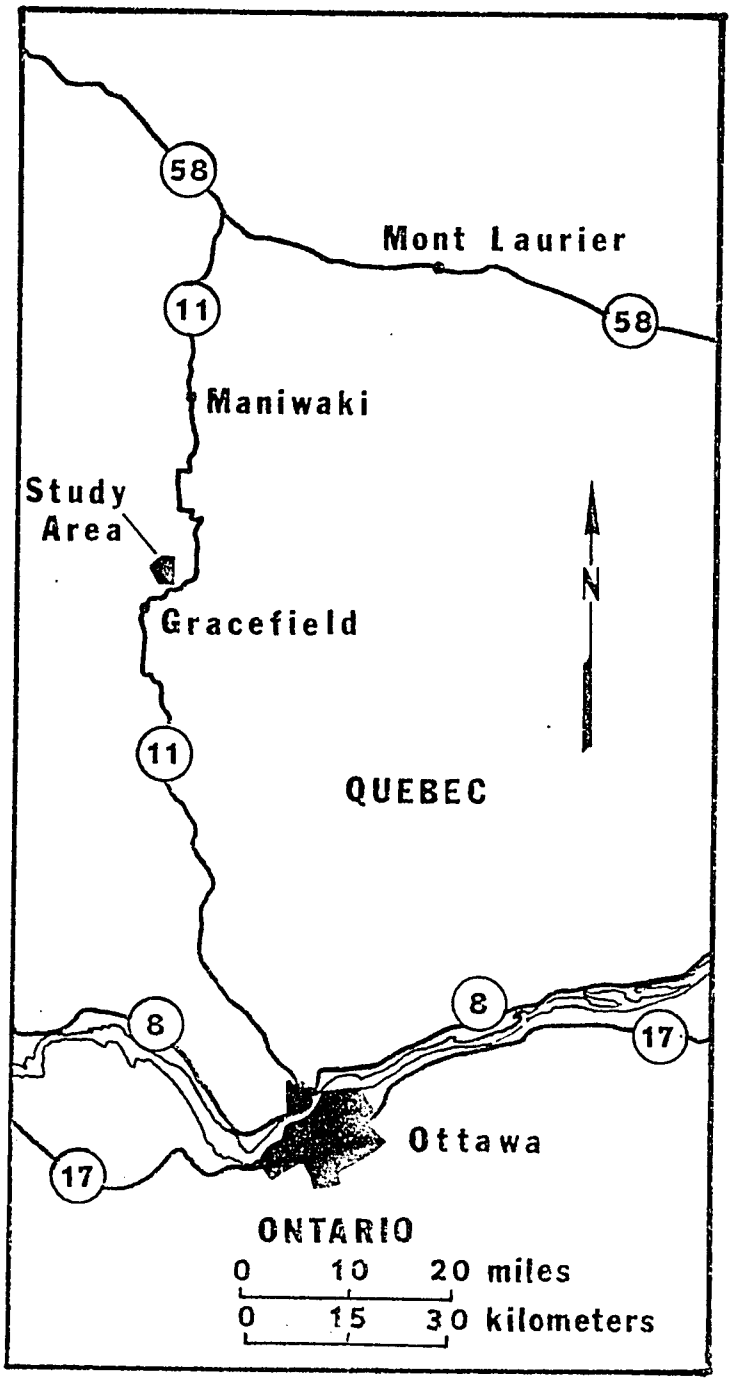

Figure 1 Index map showing the location of the study area

Previous work

The earliest geological reconnaissance was made by Lewis R. Ord and Henry G. Vennor in 1876, and a description accompanied by a 1 inch to 4 miles map was published in the Geological Survey of Canada's Report for 1876-1877 (Vennor 1978). The area was later included in R.W. Ells geological report and 1 inch to 4 miles map (Ells 1907).

Aubert de la Rue (1956), described the geology of the eastern half of the area presently being studied, in his report on the "Trente-et-un Miles Lake Area".

Wynne-Edwards et al.(1966), in a large mapping survey included the study area as part of a much larger area extending to the east and north.

Bourne (1970), described the geology of the western half of the study area in his report on the "Cayamant Lake Area".

Baer (1974, personal communication), in a compilation and mapping study also included the study area as part of a larger area extending to the east, west, and north.

Geological setting of the study area based on previous data

The study area lies in a north-south trending belt of

marbles and gneisses (Figure 2). In the western part of the region the rocks consist mainly of undivided paragneisses and biotite gneisses with minor interbeds of marble, and biotite-garnet-sillimanite-feldspar gneiss (Bourne 1970, and Baer 1974, personal communication).

In the central and eastern parts of the region, the rocks consist mainly of marble with a few lenticular bodies of quartzite and biotite gneiss, which have been intruded by several syenite, gabbro, and mangerite plutons (Aubert de la Rue 1953, 1956, and Wynne-Edwards et al. 1966).

The region is characterized by northeast plunging folds. Axial plane foliations generally strike north-northeast, and dip moderately to the southeast. Most of the rocks in the region have been more-or-less affected by high-grade metamorphism (Wynne-Edwards et al. 1966).

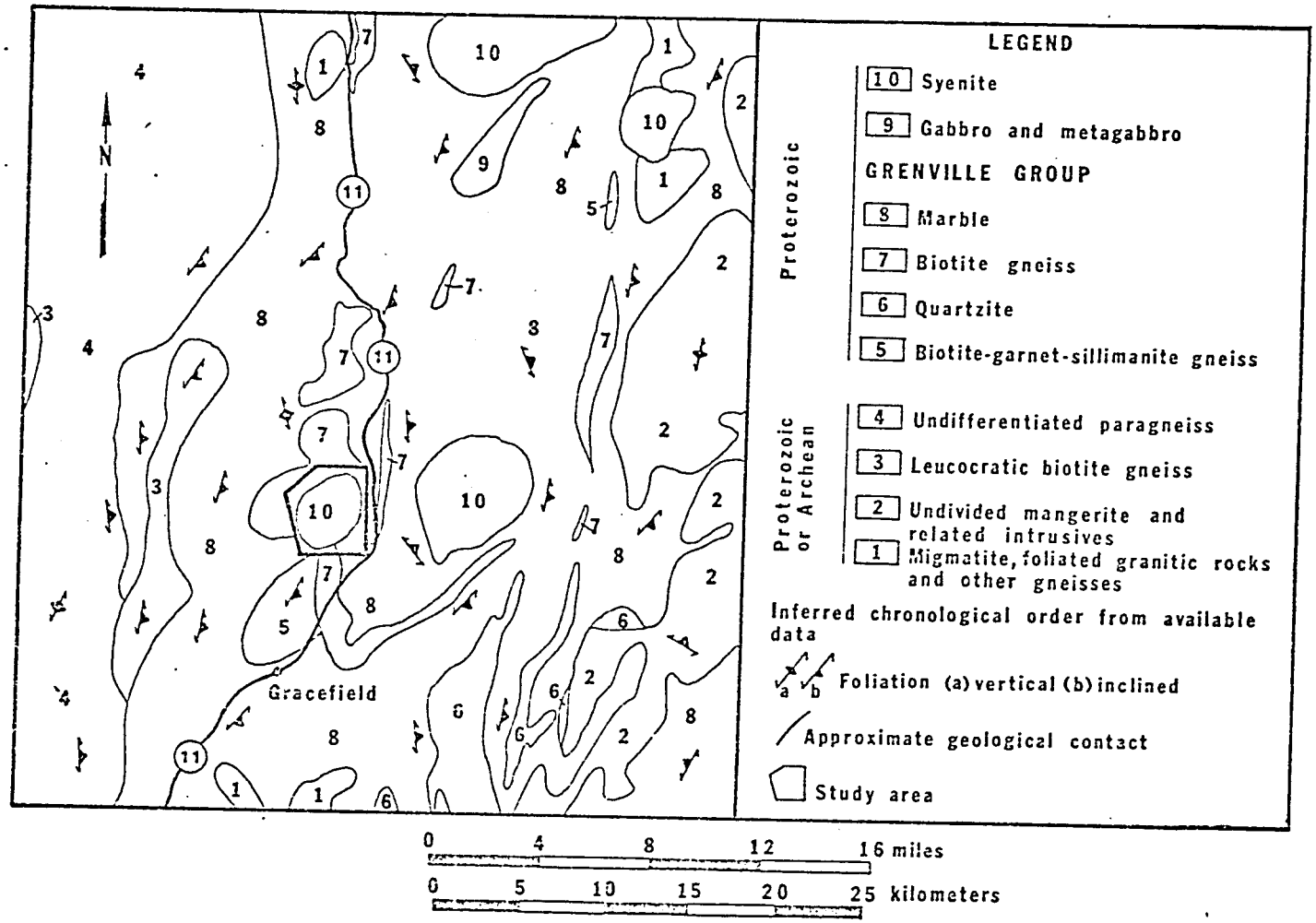

Figure 2 Map showing the geological setting of the study area (Geology after Wynne-Edwards et al. 1966, and Baer 1974 personal communication)

Note: units 1 to 4 and 5 to 8 are not necessarily in chronological order.

Equipment and methods employed during the investigation

Field work in the study area was carried out during the 1972 and 1973 spring seasons. The area is readily accessible by automobile along several secondary roads branching out from route 11, and by ground traverses between the numerous logging roads in the area.

The optical properties of the minerals were determined using a Zeiss polarizing microscope. 2V angles were measured using a Zeiss polarizing microscope with a universal stage attachment.

Modal analyses were made with a Swift point counter attached to a Zeiss polarizing microscope. In order to determine the minimum number of points required, modal analyses of two representative specimens of both syenites I and II were calculated using 1000, 1200, and 1400 points. The results are listed in Table I. All of the modal analyses used in the construction of the isopleth maps were calculated using 1400-2300 points, depending on the area of the thin section.

Chemical analyses of rocks of syenites I and II were made with the following instruments and methods. Iron, magnesium, calcium, potassium, sodium, and aluminium were determined by means of atomic absorption using a Techtron spectrophotometer. Titanium and silicon were determined

TABLE I

MODAL ANALYSES OF SELECTED SPECIMENS OF SYENITES I AND II

SYENITE I

number of points counted	1000	1200	1400	1000	1200	1400
mineral	specimen MD-121			specimen MD-113		
microperthite	82.5%	80.7%	80.5%	27.9%	26.6%	26.3%
biotite	10.1%	9.6%	9.8%	6.9%	7.8%	8.0%
barkevikite	3.1%	3.8%	3.8%	12.0%	11.1%	10.6%
apatite & epidote	1.9%	2.4%	2.3%	6.1%	7.1%	7.4%
magnetite & ilmenite	2.4%	3.0%	3.0%	7.5%	8.3%	8.6%
calcite	----	0.5%	0.7%	0.2%	0.9%	0.9%
salite	----	----	----	39.4%	38.2%	38.0%
total	100.0	100.0	100.0	100.0	100.0	100.0

SYENITE II

number of points counted	1000	1200	1400	1000	1200	1400
mineral	specimen MD-65			specimen MD-50		
microperthite	64.0%	62.8%	62.9%	62.4%	61.3%	61.0%
biotite	9.2%	9.8%	9.6%	11.3%	11.8%	12.0%
barkevikite	0.3%	0.6%	0.9%	----	0.2%	0.3%
apatite & epidote	4.2%	4.6%	4.8%	3.8%	4.4%	4.5%
magnetite & ilmenite	9.8%	10.6%	10.4%	7.9%	7.9%	8.1%
salite	12.3%	11.1%	10.7%	14.6%	14.4%	14.1%
sphene	0.2%	0.5%	0.7%	----	----	----
total	100.0	100.0	100.0	100.0	100.0	100.0

colorimetrically, using a Unicam SP 600 spectrophotometer. The Fe^{+2} content was determined using the titration method developed by Jen (1973). The P_2O_5 and CO_2 contents were calculated from modal analyses, and the remaining volatiles determined by the loss on ignition method (L.O.I.).

Several grains of barkevikite, salite, biotite, microperthite, nepheline, magnetite, and ilmenite were analysed for their major constituents using an Acton(Cameco) electron microprobe. The instrument is housed in the Geology Department, M^{c}Gill University. Natural mineral standards were used and the data were reduced using the program of Rucklidge and Gasparrini (1969).

Each mineral analysis represents the average of 10 spot analyses taken on the same grain. In the case of salite, barkevikite, and biotite, the analyses were taken so as to provide traverses across the crystals. In the case of microperthites, a broad beam was used to determine as closely as possible the bulk composition of the grains.

The components in the pyroxene were calculated by the University of Oslo proceedure, based on a method suggested by Essene and Fyfe (1967). The amphibole and biotite formulae were calculated on the basis of 46 and 44 positive charges respectively. The partitioning of Fe^{+2} and Fe^{+3} in the magnetites is based on the following formula:

$8(Fe^{+2},Mg)(Fe^{+3},Ti)_2O_4$. The magnetite formulae were calculated assuming 32 oxygens and 24 cations total. Similarly, the partitioning of Fe^{+2} and Fe^{+3} in ilmenite is based on the following formula: $Fe^{+2}_{1-x}\ Fe^{+3}_{2x}\ Ti_{1-x}\ O_3$. The ilmenite formulae were calculated assuming 6 oxygens and 4 cations total. The low cation totals reported in Table VII are due to the fact that not all of the cations analysed were reported by the data reduction program. The alkali feldspar and nepheline formulae were calculated on the basis of 32 oxygens. Modified C.I.P.W. norms were calculated using a computer program, developed by Pierre Lapointe, at the University of Ottawa.

Acknowledgements

The author whishes to thank Dr. D.D. Hogarth for his supervision of the field and laboratory investigations and for his guidance and helpful criticisms during the writing of the thesis.

The author also wishes to thank Dr. R. Kretz, Dr. W.K. Fyson, and Dr. A. Baer of the Geology Department of the University of Ottawa, and Dr. K. Currie of the Geological Survey of Canada, for reading the thesis, and for their helpful suggestions and criticisms.

Thanks are also extended to Mr. E. Hearn for photographing the thin sections, and for the plates exhibited in the thesis. Thanks are also extended to Mrs. D. Garett for assistance in doing the chemical analyses, Carlos de la Fuente for his assistance during the X-Ray investigations, Pierre Lapointe for the use of his computer program,,and Tarig Ahmedali of the Geology Department, M^{c}Gill University, for his assistance during the electron microprobe analyses.

The author also wishes to thank his wife for her encouragement during the writing of the thesis.

CHAPTER II

GEOLOGY OF THE STUDY AREA

The rocks of the study area consist of a sequence of marbles and paragneisses, which have been intruded by the Gracefield syenite pluton.

In the northern, western, and southern parts, the country rocks consist mainly of calcitic marbles with a few lenticular bodies of feldspathic quartzite and biotite-feldspar gneiss, whereas in the eastern part of the area, they consist mainly of paragneisses* (Figure 3). The syenite pluton is roughly oval in shape, and is composed of two distinct syenite intrusions. The earliest intrusive, will be referred to in the text, as syenite I, and the later one as syenite II (Figure 3).

The foliation of the surrounding metasedimentary rocks generally strikes north-northeast, and dips moderately to the east except near the syenite pluton, where it tends to parallel the contact between the pluton and the adjacent country rocks. Along the western contact of the pluton, the foliation in the country rocks dips shallowly to moderately inward toward the pluton, whereas along the eastern contact the foliation dips away from the pluton (Figure 3).

*terminology of Bourne (1970)

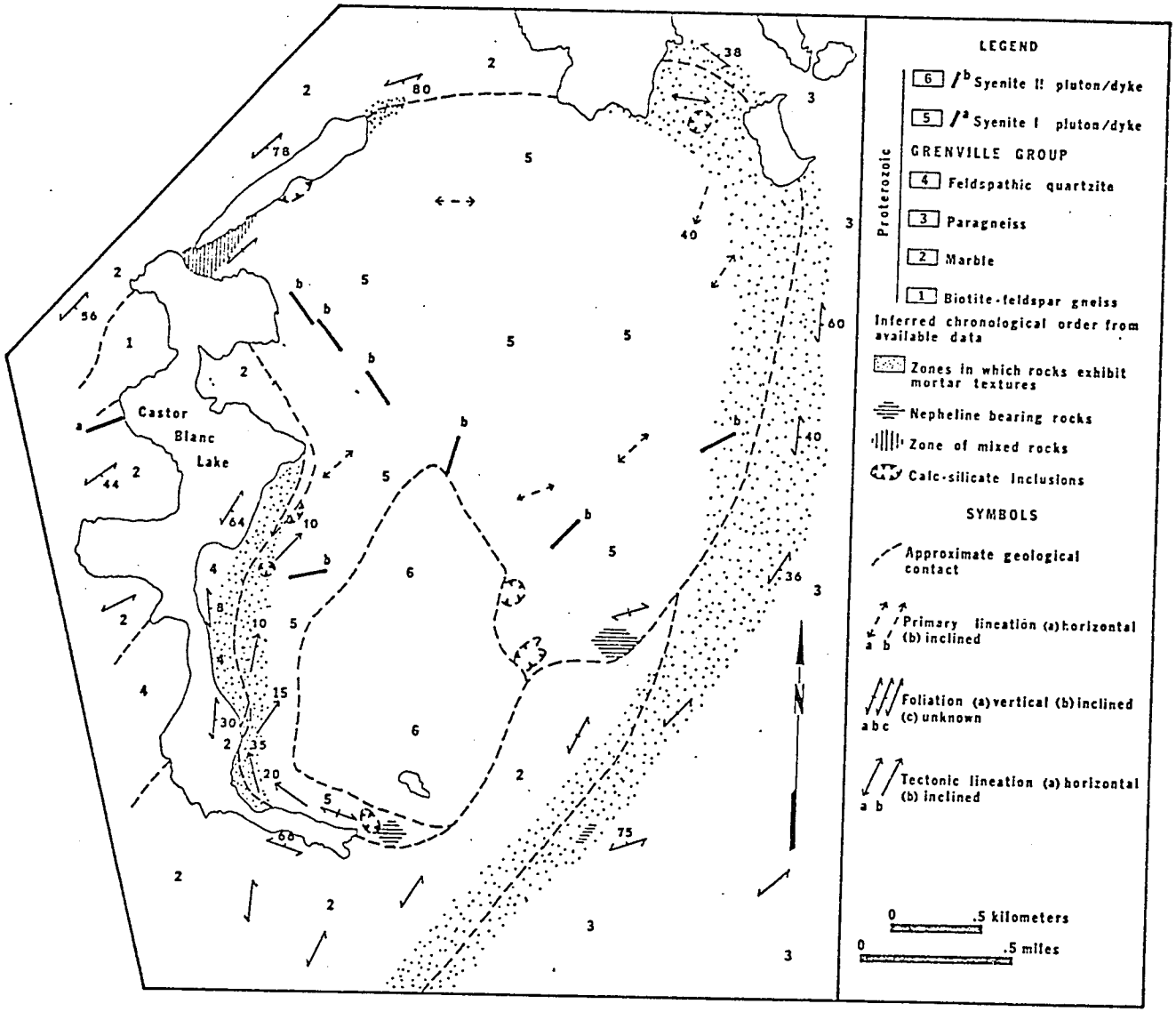

Figure 3 Map showing the geology of the study area

All the rocks in the study area except those of the syenite pluton have been subjected to regional high grade metamorphism. The rocks of the Gracefield pluton do not appear to have been highly metamorphosed.

Biotite-feldspar gneiss

In the northwest part of the study area, there is a lenticular body of gneissic rocks (Figure 3). Bourne (1970), mapped these rocks as hornblende gneisses. They are dark grey, fine grained, and composed of 75% K-feldspar, 22% biotite, 3% plagioclase, and trace amounts of diopsidic pyroxene, sphene, and opaques.

In the northern part of this unit, there is a zone of mixed rocks (Figure 3). In the eastern part of this zone, the rocks consist of a massive, medium to coarse grained, K-feldspar rich syenite which contains a few thin contorted bands of fine grained gneissic rocks. These rocks grade westwardly into thinly bedded gneisses which contain a few small sill/dyke-like bodies of syenite.

These rocks are described in this section rather than in the section under syenite I, because the relict bands of gneissic rocks are structurally continous with, and mineralogically similar to the gneissic rocks southwest of the zone of mixed rocks (Figure 3). Several of these relict bands

have been partially assimilated, and there has been segregation of mafic and felsic minerals (Plate 1).

Marble

These rocks are generally medium to coarse grained, and composed mainly of twinned calcite with minor amounts of phlogopite, graphite, apatite, sphene, tremolite, and forsterite. Foliation is poorly developed, and defined by thin discontinous zones in which phlogopite and graphite flakes have a parallel alignment. However, in some outcrops the foliation is defined by thin zones, which are rich in apatite and sphene.

In one locality, near the western contact of the pluton, the marbles have been altered to calc-silicate rocks, which are composed mainly of diopsidic pyroxene and minor amounts of calcite. Deformation twins, bent twins, and mortar textures in calcite, were observed in several thin sections.

Paragneiss

These rocks are light grey in color, fine to medium grained, and composed of 80-95% K-feldspar, 4-15% biotite and minor amounts of plagioclase, garnet, sphene, magnetite, and nepheline in one locality. Bourne (1970), reported sillimanite in rocks of this unit, but none was observed in the thin sections examined. In all the thin sections examined, these rocks exhibit mortar textures (Plate 2).

Feldspathic quartzite

In the southwest part of the thesis area, there is what appears to be a lenticular body of quartzo-feldspathic rocks (Figure 3). Bourne (1970), mapped these rocks as meta-arkoses. They are grey to greyish pink in color, and fine to medium grained. These rocks are composed of 85-95% quartz, 5-15% K-feldspar and plagioclase, and minor amounts of biotite, opaques, and sphene. Close to the syenite pluton these rocks exhibit mortar textures.

Distribution and relationships between syenites I and II

Syenite I makes up most of the Gracefield pluton and has an area of approximately 3 square miles (Figure 3). Syenite II is a pear shaped body, which is approximately 1 square mile in area, and occupies the southern part of the pluton (Figure 3). Except for the southeastern part, where it is in contact with marble, syenite II is completely enclosed by syenite I (Figure 3).

During the field work, several dykes of syenite II cutting across the rocks of syenite I were observed. These dykes vary in width from 10 to 20 feet, and seem to form a pattern radiating out from syenite II (Figure 3). Also, in one locality there is a sharp intrusive contact between the two syenites. At this same locality, there are partially

resorbed angular fragments of syenite I in syenite II. Elsewhere, in the vicinity of syenite II, the rocks of syenite I are highly fractured. These observations indicate that syenite II is the younger of the two, and that it has intruded syenite I.

Syenite I

These rocks are holocrystalline, and hypidiomorphic. They are medium to coarse grained, and there does not appear to be any variation in grain size across the intrusion The color is light pink except in the central part of the intrusion where it is greenish black and near the contact with syenite II, where it is light grey.

The mineralogical composition of syenite I is quite variable. It is composed of 0-38% salite, 0-40% barkevikite, 2-30% biotite, 26-85% microperthite, 0-2% plagioclase, tr.-9% apatite, tr.-3.5% calcite, tr.-8.5% magnetite and ilmenite, and trace amounts of sphene, epidote, and zircon.

The central part of the intrusive is rich in mafic and poor in felsic minerals, and corresponds to shonkinite. The rocks close to the borders of the intrusion are rich in felsic and poor in mafic minerals, and correspond to alkaline syenites. There appears to be a complete gradation between these two rocks types. The alkali syenite is locally transitional

to nepheline syenite (Figure 3), which is composed of 9-15% biotite, 67-70% microperthite, 11-21% nepheline, 1-2% magnetite and ilmenite, and trace amounts of sphene, calcite, epidote, and zircon.

In one locality, on the western shore of Castor Blanc Lake, a dyke of quartz syenite cuts marble (Figure 3). This dyke is tentatively correlated with syenite I.

Syenite I contains several calc-silicate inclusions along its margins, and near syenite II (Figure 3). They are generally quite large, and may have diameters of several hundred feet. They are composed of 13-59% diopsidic pyroxene, 2-26% hornblende, 0-30% biotite, 16-40% K-feldspar, tr.-6.7% magnetite, tr.-3% calcite, and trace amounts of sphene.

A primary foliation interpreted as igneous was observed in the nepheline-bearing rocks. The primary foliation is parallel to the borders of the intrusion (Figure 3), and is defined by tablets of K-feldspar which have a parallel orientation. Horizontal or nearly horizontal primary igneous lineations defined by K-feldspar laths, were observed and measured in several localities (Figure 3).

In several places along the margins of the intrusion, the rocks exhibit mortar texture. This texture consists of

relict, spindle-shaped fragments of rock composed of microperthite, barkevikite, salite, magnetite, and biotite in a fine grained matrix of recrystallized K-feldspar, plagioclase, and biotite (Plate 3). These spindle-shaped fragments define horizontal or nearly horizontal lineations (Figure 3). In several places this texture is only incipiently developed along grain boundaries, and does not define lineation.

Syenite II

These rocks are also holocrystalline and hypidiomorphic. They are greenish brown in color, and are variable in grain size. They are fine grained at the margins of the intrusion, and progressively become medium grained in the central part of the intrusion.

Syenite II is composed of 0-31% salite, 0-13% barkevikite, 3-19% biotite, 40-80% microperthite, 2-11% magnetite and ilmenite, 2-6.5% apatite, 0-8% plagioclase, 0-1.5% calcite, and trace amounts of sphene, epidote, and zircon.

Generally, the rocks in the central part of syenite II are richer in mafic and poorer in felsic minerals than the rocks near the margins of the intrusion. However, this trend is not as regular or as well defined as the trend in syenite I.

The dykes of syenite II which cut across the rocks of syenite I, are composed approximately of 14% salite, 15% biotite, 60% microperthite, 7% magnetite and ilmenite, 3% apatite, and trace amounts of plagioclase.

Shape of the Gracefield pluton

From surficial geological mapping, the Gracefield pluton is roughly oval in shape. Foliations in the country rocks near the southern, western, and northern contacts of the pluton, dip inwards, toward the pluton. Along the eastern contact, the foliations dip away from the pluton (Figure 3).

The aeromagnetic map of the area (map 225G, Department of Mines and Technical Surveys, Ottawa) shows that the pluton has a positive magnetic anomaly. Superimposing the two maps reveals that the western contact of the pluton corresponds quite closely with the 1500 gamma contour. However, the magnetic anomaly extends considerably farther east than the eastern contact of the pluton (Figure 4). The foliation pattern, and the shape of the magnetic anomaly, suggest that the pluton has the shape of an inclined pipe, plunging eastwardly.

Position of the Gracefield pluton in the Grenville tectonic and metamorphic history

Several lines of evidence seem to suggest that syenites I and II were intruded late in the Grenville metamorphic and tectonic history. These are:

1) the foliation in the surrounding country rocks is well developed, and does not penetrate into the pluton (Figure 3).
2) relict igneous textures such as large, well formed, singly twinned K-feldspar crystals are common.

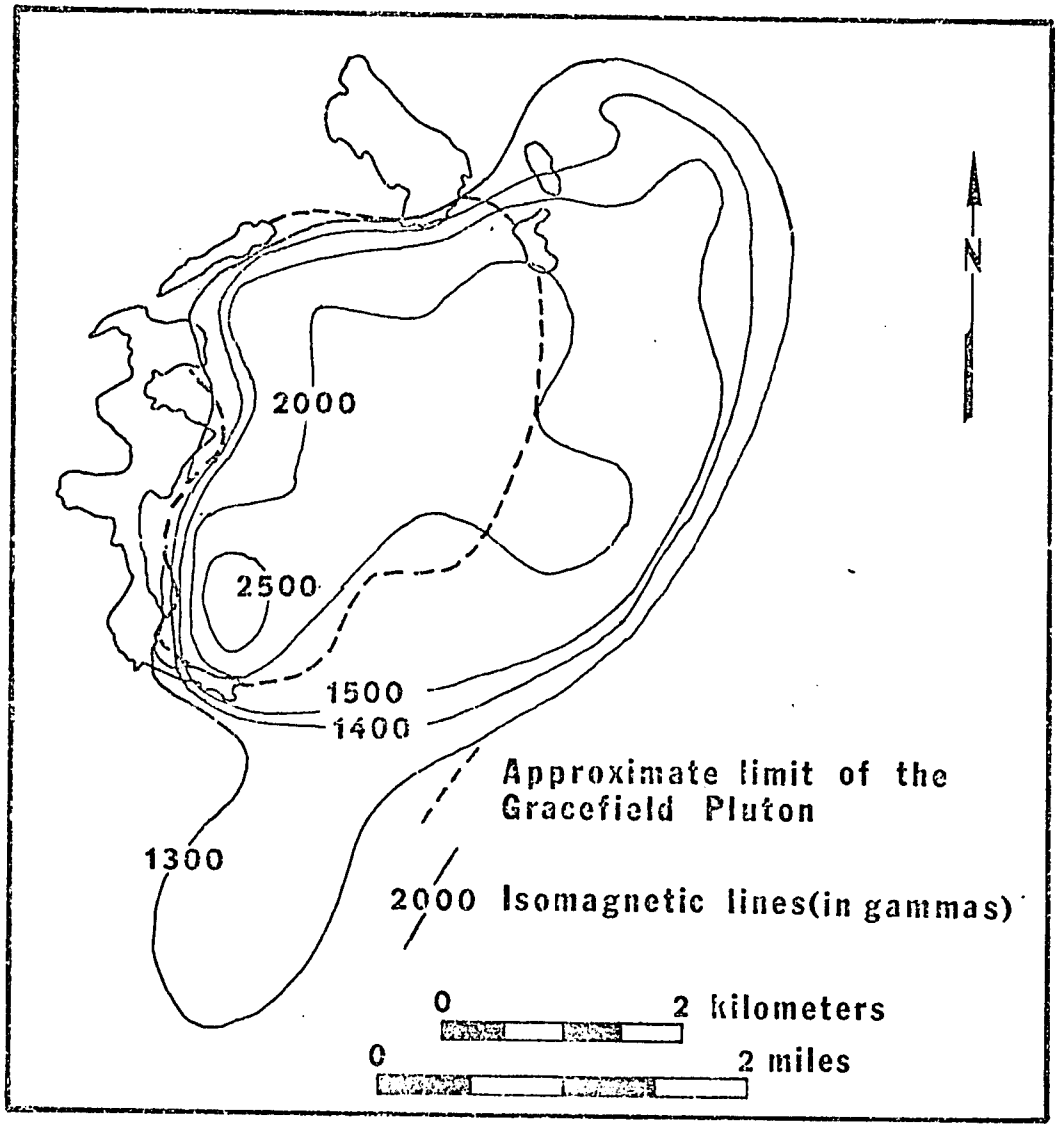

Figure 4 Diagram showing the relationship between the Gracefield pluton and its aeromagnetic anomaly. Isomagnetic lines taken from Aeromagnetic Map 225G, Department of Mines and Technical Surveys, Ottawa.

3) in the northwest part of the study area, syenite I contains several partially assimilated bands of gneissic rocks (Figure 3).

4) the age of the similar Kensington syenite, which is approximately 25 miles north of the study area was determined by the K-Ar method to be 884 m.y. by Doig and Barton (1968). However, this is a minimum age, and may represent the date of waning metamorphism.

5) that the magma intruded gneisses and marbles without producing a noticeable thermal aureole, and that there are no chilling effects in syenite I. This suggests, that the magma was not very different in temperature from that of the host rocks at the time of intrusion.

6) in the study area, there are two north-south trending zones in which the rocks exhibit mortar textures. These zones are mainly confined to the paragneiss, and feldspathic quartzite units, but they also extend across the northeastern and southwestern parts of the Gracefield pluton (Figure 3). Although there is generally some recrystallization, these textures are usually developed in relatively cold rocks, during the late stages of deformation (Spry, 1969). In this case, during deformation, the relatively brittle and competent syenitic, quartzitic, and gneissic rocks appear to have deformed cataclastically, whereas the relatively incompetent marbles appear to have deformed plastically.

CHAPTER III

MINERALOGY AND TEXTURES OF SYENITES I AND II

Salite

Optical properties. The clinopyroxenes in syenites I and II have similar optical properties. They correspond to those of salite, but there is some overlap with those of titanaugite. They are optically positive, have $2V_z$ angles between 55-60°, and extinction angles between 36° and 42°. In thin section they are very pale green and weakly pleochroic with X=pale green, Y=pale greyish green, and Z=brownish green. Some salites are zoned optically, with $Z \wedge c$(core) 42°, dispersion strongly inclined about $Y(Z_v \wedge c > Z_r \wedge c)$, and $Z \wedge c$(rim) 35°, dispersion weakly inclined about Y.

Chemistry. Several clinopyroxene grains from the central and marginal parts of syenites I and II were analysed for the major elements using an electron microprobe. The results are presented in Table II.

Examination of these results does not reveal any major difference in chemistry between the clinopyroxenes of syenites I and II. Most are aluminous titanian salites. One specimen (MD-113) contains an appreciable amount of calcium Tschermak's molecule ($CaAl[SiAl]O_6$) and as such is better classified as a titanian fassaite. For convenience, all pyroxenes in these syenites will be termed salites.

TABLE II

CHEMICAL COMPOSITION OF SALITES OF SYENITES I AND II

intrusive	SYENITE I			SYENITE II		
specimen no	MD-113	MD-22 1&2		MD-30 1&2		MD-62
location	center	margin		center		margin
oxides	oxides	oxides		oxides		oxides
SiO_2	49.34	52.50	50.68	51.54	50.26	51.61
TiO_2	1.77	0.79	1.47	0.93	1.16	0.83
Al_2O_3	6.85	4.51	6.82	5.04	5.08	3.82
FeO*	7.84	9.08	9.57	8.07	9.32	8.77
CaO	21.52	21.33	21.12	21.33	20.46	20.71
MgO	12.46	11.01	9.96	12.06	11.98	11.70
Na_2O	1.34	1.73	1.80	0.76	0.96	1.43
K_2O	-----	-----	-----	-----	0.04	0.01
total	100.13	100.96	101.42	99.73	99.27	98.88
FeO/MgO(wt)	0.63	0.82	0.96	0.67	0.77	0.75

*all iron reported as FeO

FORMULAE BASED ON 4.00 CATIONS

	MD-113		MD-22(1)		MD-22(2)		MD-30(1)		MD-30(2)		MD-62	
Si	1.802	2.00	1.933	2.00	1.863	2.00	1.923	2.00	1.886	2.00	1.939	2.00
Al^{iv}	0.198		0.067		0.137		0.077		0.114		0.061	
Al^{vi}	0.097	1.06	0.129	1.03	0.159	1.04	0.145	1.09	0.111	1.11	0.108	1.06
Ti	0.049		0.021		0.041		0.026		0.033		0.023	
Fe	0.239		0.280		0.294		0.252		0.292		0.276	
Mg	0.678		0.604		0.546		0.671		0.670		0.655	
Ca	0.842	0.94	0.842	0.97	0.832	0.96	0.852	0.91	0.823	0.89	0.834	0.94
Na	0.095		0.124		0.128		0.055		0.070		0.104	
K	-----		-----		-----		-----		0.002		-----	

END MEMBERS IN MOLECULAR PERCENT

	MD-113	MD-22(1)	MD-22(2)	MD-30(1)	MD-30(2)	MD-62
$CaTiAl_2O_6$	4.85	2.17	4.06	2.70	3.27	2.34
$CaAl[SiAl]O_6$	10.07	2.27	5.53	2.61	4.87	1.44
$NaAlSi_2O_6$	-----	10.52	10.36	5.68	6.19	9.34
$NaFe^{+3}Si_2O_6$	9.47	1.72	2.47	-----	0.99	1.12
$Ca_2Si_2O_6$	34.56	39.50	36.8[illegible]	41.38	37.06	39.78
$Fe^{+2}_2Si_2O_6$	7.21	13.85	13.48	13.00	14.13	13.22
$Mg_2Si_2O_6$	33.84	29.95	27.29	34.64	33.50	32.75

Table II also reveals that there are smallvariations in the chemical compositions of salites within the two syenite bodies. The FeO/MgO(wt) is moderate (0.63) in salite from the central part of syenite I, and higher (0.82,0.96) in salites from the marginal rocks of the intrusion. In syenite II this ratio does not vary significantly. The Al_2O_3 content is higher in salites from the central parts of syenite II, than in salites from the borders of the intrusion; whereas in syenite I, it does not appear to vary significantly. The other elements do not appear to vary significantly within salites from the two intrusions. The analysed salites were not optically zoned; several microprobe traverses across the grains did not reveal chemical zoning.

Textures. In syenites I and II, salite occurs as small subhedral to anhedral grains, which display a variety of textures. In the central part of syenite,I and in the southern part of syenite II salite occurs in cumulus like aggregates. Barkevikite, microperthite, magnetite, and ilmenite occur interstitially between salite crystals, and often include them (Plates 4 and 5). In the marginal rocks of syenite I,and in most of syenite II, salite occurs as small anhedral, interstitial crystals between the larger microperthite crystals (Plate 6). In most of the thin sections examined, salite grains were partially or completely rimmed by barkevikite and biotite grains (Plate 7).

In both, syenites I and II, salite grains commonly display exsolution of magnetite along cleavage planes (Plate 8). In most of the thin sections examined, salite grains were fresh and unaltered. However, in a few places along the margins of syenite I and near syenite II, salite grains are altered to uralite (Plate 9).

Barkevikite

Optical properties. Amphiboles in syenites I and II, have optical properties which correspond to those of barkevikite. They are optically negative, have 2Vz angles between 40^{o} and 50^{o}, and extinction angles($Z \wedge c$) between 6^{o} and 11^{o}. The dispersion formula is r>v. In most thin sections they are yellow-brown and strongly pleochroic with X = pale yellow, Y = reddish brown, Z = dark brown. The amphibole in the extreme north-eastern part of syenite I has optical properties which correspond to those of hornblende.

Chemistry. Electron microprobe analyses of barkevikites from rocks in the marginal and central parts of syenite I, and from the marginal rocks of syenite II, are presented in Table III. They contain less than 0.5 Ti atom per formula unit, and are very similar to those presented by Deer, Howie, and Zussman (1963, pp 329-330).

Barkevikites from rocks in the central part of syenite I are richer in TiO_2, Al_2O_3, and Na_2O than barkevikites from rocks in the marginal parts of the same body. The SiO_2, CaO, and K_2O contents are approximately the same in barkevikites from rocks in both parts of the intrusion. Barkevikites from the marginal rocks of syenite II, are compositionally similar to those from the marginal rocks of syenite I, but they have lower FeO contents.The SiO_2, Al_2O_3, CaO, Na_2O, MgO, and K_2O contents are approximately

TABLE III

CHEMICAL COMPOSITION OF BARKEVIKITES OF SYENITES I AND II

intrusive	SYENITE I		SYENITE II
specimen no	MD-113	MD-22	MD-62
location	center	margin	margin
oxides	oxides	oxides	oxides
SiO_2	41.04	41.22	41.35
TiO_2	4.10	2.39	2.27
Al_2O_3	13.70	12.07	11.66
FeO*	12.10	15.68	14.72
CaO	11.28	11.05	11.43
MgO	12.70	11.00	11.45
Na_2O	2.85	2.39	2.34
K_2O	2.30	2.42	1.96
total	100.07	98.22	97.18
FeO/MgO(wt)	0.95	1.42	1.29

* all iron reported as FeO

FORMULAE BASED ON 46 POSITIVE CHARGES

Si	5.981	6.213	6.262
Al^{iv}	2.019 (8.00)	1.787 (8.00)	1.738 (8.00)
Al^{vi}	0.334	0.357	0.343
Ti	0.449	0.271	0.259
Mg	2.759 (5.02)	2.472 (5.08)	2.585 (5.05)
Fe^{+2}	1.475	1.977	1.864
Ca	1.761	1.785	1.855
Na^{viii}	0.239 (2.00)	0.215 (2.00)	0.145 (2.00)
Na^{xii}	0.567	0.483	0.542
K	0.428 (0.99)	0.465 (0.95)	0.379 (0.92)

the same.

The FeO/MgO ratio in barkevikite is (0.95 wt) in the central part, and considerably higher (1.42 wt) in the marginal rocks of syenite I. This ratio is also high (1.29) from the marginal parts of syenite II.

Textures. In syenites I and II, barkevikite crystals are usually associated with salite, biotite, magnetite, ilmenite, and apatite. The crystals are fresh, have variable grain size, and do not exhibit any exsolution features.

In the central part of syenite I, and southern parts of syenite II, barkevikite occurs mainly as large intercumulus like crystals. It normally encloses several grains of salite, apatite, K-feldspar, magnetite, and ilmenite. Less commonly it is found as small blebs within salite crystals (Plates 4 and 5). Also, in a few thin sections they are interstitial between larger microperthite grains (Plate 6).

In the marginal rocks of syenites I and II, barkevikite generally occurs as partial rims around, and as small blebs within salite grains (Plate 7). In most thin sections, barkevikite grains are partially rimmed with ragged biotite crystals (Plate 7).

Biotite

Optical properties. There are no differences in the optical properties of biotites in syenites I and II. They are optically negative, have 2Vx angles of about 5^{o}, and extinction angles ($Z \wedge a$) between 3^{o} and 5^{o}. The biotite flakes are black in hand specimen, and yellowish brown in thin section. They are strongly pleochroic, with X = pale yellow, Y = reddish brown, and Z = reddish brown.

Chemistry. Several microprobe analyses of biotites are presented in Table IV.
In syenite II, the FeO/MgO ratios in biotites decrease from the center to the borders of the intrusion. Conversely, in syenite I, the FeO/MgO ratios in biotites are low in the central part, and progressively increase toward the borders of the intrusion. There is also a decrease in the TiO_2, and an increase in the Al_2O_3 contents in biotites from the center to the margins of the intrusion.

Textures. In both syenites I and II, there appears to be two modes of occurrence of biotite. One of these modes, consists of small ragged crystals, which form partial rims around, and small patches within barkevikite, salite, magnetite, and ilmenite (Plates 7 and 10). They also occur as small, discreet flakes between microperthite crystals (Plate 11).

TABLE IV

CHEMICAL COMPOSITIONS OF BIOTITES OF SYENITES I AND II

intrusive	SYENITE I			SYENITE II	
specimen no	MD-113	MD-22	MD-84A	MD-30	MD-62
location	center	intermediate	margin	center	margin
oxides	oxides	oxides	oxides	oxides	oxides
SiO_2	36.89	38.38	36.37	38.37	38.03
TiO_2	6.65	3.80	4.57	4.74	4.39
Al_2O_3	14.42	13.37	18.25	13.91	13.05
FeO*	11.40	13.38	17.82	15.20	12.72
CaO	-----	0.10	-----	-----	-----
MgO	16.90	16.22	9.75	14.76	16.42
Na_2O	0.68	0.17	0.18	0.22	0.13
K_2O	9.84	8.93	9.47	8.50	9.09
total	96.77	94.86	96.56	95.67	93.82
FeO/MgO(wt)	0.67	0.82	1.82	1.03	0.77

* all iron reported as FeO

FORMULAE BASED ON 44 POSITIVE CHARGES

	MD-113		MD-22		MD-84A		MD-30		MD-62	
Si	5.378	7.86	5.728	8.08	5.424	8.63	5.673	8.10	5.701	8.01
Al	2.477		2.351		3.208		2.424		2.306	
Ti	0.729	5.80	0.426	5.70	0.512	4.90	0.527	5.66	0.495	5.76
Fe	1.389		1.670		2.223		1.879		1.595	
Mg	3.677		3.607		2.167		3.252		3.668	
Ca	-----	2.02	0.003	1.75	-----	1.85	-----	1.67	-----	1.85
Na	0.019		0.048		0.052		0.062		0.036	
K	1.829		1.699		1.801		1.603		1.737	

The second habit of biotite is as large thick sheets, consisting either of a single large crystal, or several small sheets which have parallel orientations (Plates 12 and 13). They vary in width from a few millimeters to several (4-5) centimeters, and cut across the other minerals which make up the rocks of syenites I and II; thereby imparting a cumulus-like texture to the rocks (Plate 4). Legris (1972), observed similar textures in a syenite pluton near Renfrew, Ontario.

These large flakes of biotite have random orientations (Plate 13), and are very common in the rocks of syenite II, and in the rocks of syenite I adjacent to syenite II. Farther away from syenite II, they are encountered less frequently.

Whether or not these two modes of occurrence represent two generations of biotite is not known, and further work is required to resolve this question.

Microperthite

Microperthites in syenites I and II are complex. Single crystals exhibiting both replacement and exsolution perthites are common. In crystals of replacement perthite the host mineral is orthoclase; whereas in crystals of exsolution perthite, the host mineral is usually microcline but can be orthoclase. X-ray diffraction studies on several grains of fine-grained microperthite did not yield distinctive orthoclase or microcline patterns but transitions between the two patterns, suggesting " intermediate microcline".

Optical properties. Orthoclase and microcline are optically negative, and have 2Vx angles which vary between 40° and 50°, and between 70° and 90°, respectively. They both have low birefringences and low, negative relief.

The plagioclase blebs in the replacement microperthites are optically negative, have low positive to negative relief, and have 2Vx angles which vary between 84° and 88°. They are often twinned according to the albite law, and the maximum symmetrical extinction angles with respect to the fast ray are 11° to 13°. These data correspond to anorthite contents of approximately 28-30% consistent with the chemical compositions of MD-30 and MD-62. In exsolution perthites, the exsolved plagioclase has a lower R.I. than that of Canada Balsam, but higner than that of the host mineral.

This suggests that it may be albitic in composition. The exsolution blebs are too small to determine their other optical properties.

Chemistry. The electron microprobe analyses of microperthites from syenites I and II, in Table V, represent the bulk compositions of the crystals. Examination of Table V reveals that there are major differences in chemistry between microperthites of the two intrusions. In syenite I, the percentages of K_2O are much greater than those of Na_2O, and there are only trace amounts of CaO; whereas, in syenite II, the Na_2O contents are greater than the K_2O contents, and there are considerable amounts of CaO. The Al_2O_3 content is also higher in microperthites from syenite II.

The high CaO and Al_2O_3 contents in the microperthites from syenite II, are probably due to the fact, that the analysed grains were probably replacement microperthites which were morphologically similar to exsolution microperthites.

Within syenite I, there are slight differences in chemistry between microperthites from the central and marginal parts of the intrusion (Table V). In the central part of the intrusive, they are richer in CaO and Al_2O_3, and poorer in K_2O and SiO_2. In syenite II, microperthites in the central part of the intrusion, are slightly richer in CaO and Al_2O_3, and poorer in Na_2O.

TABLE V

CHEMICAL COMPOSITION OF MICROPERTHITES FROM SYENITES I AND II

intrusive	SYENITE I			SYENITE II	
specimen no	MD-113	MD-22	MD-84A	MD-30	MD-62
location	center	intermediate	margin	center	margin
oxides	oxides	oxides	oxides	oxides	oxides
SiO_2	61.94	63.08	65.81	62.57	62.73
TiO_2	0.10	0.03	0.02	0.08	0.02
Al_2O_3	19.85	18.51	19.19	21.72	20.92
FeO*	0.10	0.08	0.03	0.13	0.09
CaO	0.76	0.14	0.13	3.22	2.22
Na_2O	3.36	2.10	3.01	6.28	7.04
K_2O	10.66	13.16	12.34	5.39	4.61
total	96.56	97.12	100.53	99.39	97.61

*all iron reported as FeO

FORMULAE BASED ON 32.00 OXYGENS

	MD-113	MD-22	MD-84A	MD-30	MD-62	
Si	11.655	11.905	11.930	11.344	11.492	
Al	4.359	4.076	4.060	4.554	4.473	
Ti	0.014	0.003	0.002	0.011	0.001	
Fe^{+2}	0.015	0.012	0.004	0.020	0.013	
Ca	0.153	0.027	0.025	0.625	0.435	
Na	1.226	0.767	1.057	2.207	2.499	
K	2.558	3.169	2.852	1.246	1.077	
	64.99	79.94	72.49	30.55	26.84	Or
	31.13	19.37	26.86	54.11	62.32	Ab mole %
	3.87	0.68	0.63	15.33	10.84	An

Textures. In the Gracefield pluton, textures exhibited by microperthite grains are varied and complex, due to the presence of both replacement and exsolution microperthites. Microperthite crystals range in size from a few millimeters to two centimeters, and are generally larger in syenite I than in syenite II. There does not appear to be any variation in grain size across syenite I, but in the marginal rocks of syenite II, microperthite grains are smaller than in other parts of the intrusion. In most thin sections, these crystals are relatively fresh, but in a few localities along the borders of syenite I, and near syenite II, they are considerably altered to sericite.

Except for a small area in the central part of syenite I, replacement perthites are found in all parts of the Gracefield pluton. They consist of irregularly shaped relict plagioclase patches enclosed by orthoclase. In syenite I, plagioclase relicts rarely exceed 1-2 millimeters in diameter, and make up 1-20% of the microperthite whereas, in syenite II, they are as large as 4 millimeters, and make up 10-50% of the microperthite grains (Plates 14 and 15).

The shapes and distribution of relict plagioclase grains within the host minerals are variable. They occur as:

a) large centrally located crystals, which have ragged and deeply embayed margins, and which are surrounded by orthoclase microperthite (Plate 15).

b) numerous small irregularly shaped patches scattered throughout the host mineral (Plates 14 and 16).
c) relatively large patches along the margins of the microperthite grains (Plates 16 and 17).
d) parallel strings and rods scattered throughout the host crystal (Plate 18).

In the last three cases the relict plagioclase patches or strings are commonly in optical continuity.

Exsolution microperthites are found in all parts of the Gracefield pluton. They consist of thin films of plagioclase set in a K-feldspar host. The plagioclase films are less than a millimeter in width, and are perpendicular to the 010 cleavage in the host crystal, and have parallel orientations (Plates 14, 15, and 17). In most crystals they are present in approximately the same proportions as the K-feldspar host.

As previously mentioned, it is not unusual to find various combinations of replacement and exsolution microperthites in single crystals (Plate 14, 16, and 17). K-feldspar crystals which do not contain any relict, or exsolved plagioclase are rare. Those which contain small amounts of plagioclase, often contain very small, randomly oriented rutile needles, which were identified optically. Legris (1972), observed the same phenomena in feldspars from a syenite intrusion near Renfrew, Ontario.

In the central part of syenite I, and the southern part of syenite II, large crystals of microperthite enclose grains of salite, apatite, (Plate 19), barkevikite, magnetite, and ilmenite. In other parts of the Gracefield pluton, microperthite grains form the framework of the rocks, the interstices of which are filled with smaller grains of microperthite, salite, barkevikite, biotite, magnetite, and ilmenite (Plates 6, 10, and 11).

Nepheline

Optical properties. It is uniaxial negative, has low negative relief, is length fast, and has parallel extinction. It has a low birefringence(0.0035), and is colorless in thin section.

Chemistry. Several nepheline crystals were analysed for the major elements using an electron microprobe. The results are presented in Table VI; along with the recalculated molecular percentages of their various components.

Textures. Nepheline is found only in the marginal rocks of syenite I (Figure 3), where it normally occurs as small subhedral crystals containing numerous cracks. It is commonly associated with small crystals of microperthite, biotite, and ore minerals, which fill the interstices between much larger microperthite crystals (Plate 20). It also occurs as small rounded inclusions in large microperthite grains. The nepheline inclusions are normally surrounded by a thin rim of albitic plagioclase (Plate 21).

TABLE VI

CHEMICAL COMPOSITIONS OF NEPHELINES FROM SYENITE I

specimen no	MD-84A-1	MD-84A-2
oxides	oxides	oxides
SiO_2	41.99	41.52
TiO_2	0.01	0.02
Al_2O_3	33.96	33.71
FeO*	0.01	0.01
CaO	0.66	0.52
MgO	0.04	0.01
Na_2O	16.28	16.20
K_2O	5.43	5.86
total	98.38	97.88

*all iron reported as FeO

FORMULAE BASED ON 32.00 OXYGENS

Si	8.191	8.167
Ti	0.001	0.001
Al	7.732	7.737
Fe^{+2}	0.001	0.001
Ca	0.137	0.109
Mg	0.011	0.002
Na	6.159	6.177
K	1.350	1.470

END MEMBERS IN MOLECULAR PERCENT

Nepheline	73.26	73.10
Kalsilite	16.13	17.46
Quartz	8.96	8.13
Anorthite	1.63	1.28

Ore minerals

Optical properties. In syenites I and II, the ore minerals consist mainly of magnetite, and minor amounts of ilmenite, which in syenite II contains lamellae of titanohematite. Magnetite is isotropic and has a low reflectance. Ilmenite has a lower reflectance than magnetite, and is anisotropic. Under crossed polars in reflected light, the colors vary from greenish grey to brownish grey. The lamellae of titanohematite, have a higher reflectance than ilmenite, and are also anisotropic. In reflected light, the colors vary from black to whitish grey.

Chemistry. Several microprobe analyses of coexisting magnetite and ilmenite are presented in Table VII. Examination of these analyses does not reveal any significant differences in the chemical composition of magnetites from syenites I and II. A study of the ilmenite analyses reveals that those in syenite I, are richer in TiO_2, and slightly poorer in MgO, than those in syenite II. The exsolved lamellae in ilmenites in syenite II, correspond chemically to titanohematite (Table VII).

Textures. In the Gracefield pluton, magnetite and ilmenite are usually closely associated with salite, barkevikite, and biotite. In the central part of syenite I, and in the southern part of syenite II, small irregular grains of of magnetite and ilmenite fill the interstices between these

TABLE VII

CHEMICAL COMPOSITIONS OF ORE MINERALS FROM SYENITES I AND II

MAGNETITE

intrusive	SYENITE I				SYENITE II	
specimen no	MD-113	MD-22-1	MD-84A 1&2		MD-30	MD-62
location	center	margin	margin		center	margin
Fe_2O_3	65.78	64.91	65.84	67.69	66.77	66.83
FeO	30.48	30.10	30.53	31.38	30.96	30.98
MgO	0.14	0.11	0.02	-----	0.11	0.03
TiO_2	0.05	0.06	0.10	-----	0.05	0.05
total	96.45	95.18	96.49	99.26	97.89	97.89

FORMULAE BASED ON 32.00 OXYGENS AND 24.00 CATIONS

	MD-113		MD-22-1		MD-84-1		MD-84A-2		MD-30		MD-62	
Fe^{+3}	15.821	15.83	15.822	15.84	15.835	15.86	15.821	15.86	15.826	15.84	15.846	15.86
Ti	0.012		0.014		0.023		0.043		0.012		0.013	
Mg	0.055	8.17	0.053	8.22	0.008	8.18	-----	8.16	0.051	8.21	0.011	8.18
Fe^{+2}	8.160		8.163		8.170		8.159		8.163		8.172	

ILMENITE

intrusive	SYENITE I		SYENITE II		TITANOHEMATITE SYENITE II
specimen no	MD-113	MD-84A	MD-30	MD-62	MD-30
location	center	margin	center	margin	center
	oxides	oxides	oxides	oxides	oxides
Fe_2O_3	2.86	2.21	9.29	7.93	85.72
FeO	40.48	41.15	37.66	37.47	-----
MgO	0.96	0.28	0.76	1.16	2.04
TiO_2	52.50	53.64	48.85	48.60	11.99
total	96.80	97.28	96.56	95.16	99.75

FORMULAE BASED ON 6.00 OXYGENS AND 4.00 CATIONS

	MD-113	MD-84A	MD-30	MD-62
Fe^{+3}	0.109	0.083	0.356	0.308
Ti	2.037	2.051	1.980	1.965
Mg	0.007	0.021	0.058	0.090
Fe^{+2}	1.747	1.749	1.621	1.634

minerals, and sometimes occur as inclusions within the minerals (Plates 4,5,7,10, and 19). Elsewhere, small anhedral grains are distributed along grain boundaries of other minerals (Plates 11 and 12).

Ilmenite grains commonly have partial rims of sphene and calcite, and in syenite II, contain exsolution lamellae of titanohematite.

Apatite

Optical properties. It is uniaxial negative, has moderate-positive relief, and has a birefringence of approximately 0.005. In hand specimen it is greyish white, and in thin section it is colorless.

Textures. In the central, northwestern, and southwestern parts of syenite I, and in a few areas in syenite II, apatite occurs as large to small subhedral to anhedral crystals which are closely associated with salite, barkevikite, biotite, and ore minerals. It occurs interstitially between these minerals and as inclusions within them (Plates 4,5,9, and 10). Elsewhere in the pluton, apatite crystals are generally smaller, but otherwise have similar modes of occurrence as those described above.

Calcite

Optical properties. It is uniaxial negative, has moderate positive to low negative relief, and high birefringence. It also has well developed $\{10\bar{1}1\}$ cleavage planes.

Textures. In the Gracefield pluton, calcite occurs as small, irregularly shaped interstitial crystals, and as a very fine-grained alteration product of plagioclase in microperthites.

Sphene

Optical properties. It is optically positive, and has 2Vz angles of approximately 30°. Z∧c angles are approximately 38°. It has very high-positive relief, and birefringence. It is faintly pleochroic in some cases with X= yellow, and Z=yellowish brown.

Textures. Sphene usually occurs as small rounded crystals which are invariably associated with ilmenite and calcite crystals. In many thin sections they form partial rims around, and penetrate into ilmenite grains.

Epidote

Optical properties. It is biaxial negative, with 2Vx angles of approximately 80°. It also has a high positive relief, and a birefringence of approximately 0.045. It is colorless in thin section.

Textures. Epidote occurs as plagioclase-epidote symplectites around biotite grains.

CHAPTER IV

DISTRIBUTION OF MINERALS IN SYENITES I AND II

Modal analyses of 84 specimens from syenites I and II, were made in order to determine the distribution of essential and accessory minerals within the two intrusives. The sample localities are shown in Figure 5.

The data were used to make isopleth maps for salite, barkevikite, biotite, microperthite, magnetite(plus minor amounts of ilmenite), apatite, and calcite. Although the results for syenites I and II are shown on the same isopleth map, values in syenite II were ignored while contouring values in syenite I, and vice versa, because they are two separate, and distinct intrusions.

Salite

Generally, in syenite I, concentrations of salite are high in the central part of the intrusion, and decrease gradually toward the margins of the body, where they are present in trace amounts or absent altogether (Figure 6). However, there are several exceptions to this general rule; for example, in several places, the marginal rocks contain high concentrations of salite (Figure 6).

In syenite II, the concentration of salite is high in the southeast part of the intrusion and gradually decreases towards the margins of the body (Figure 6).

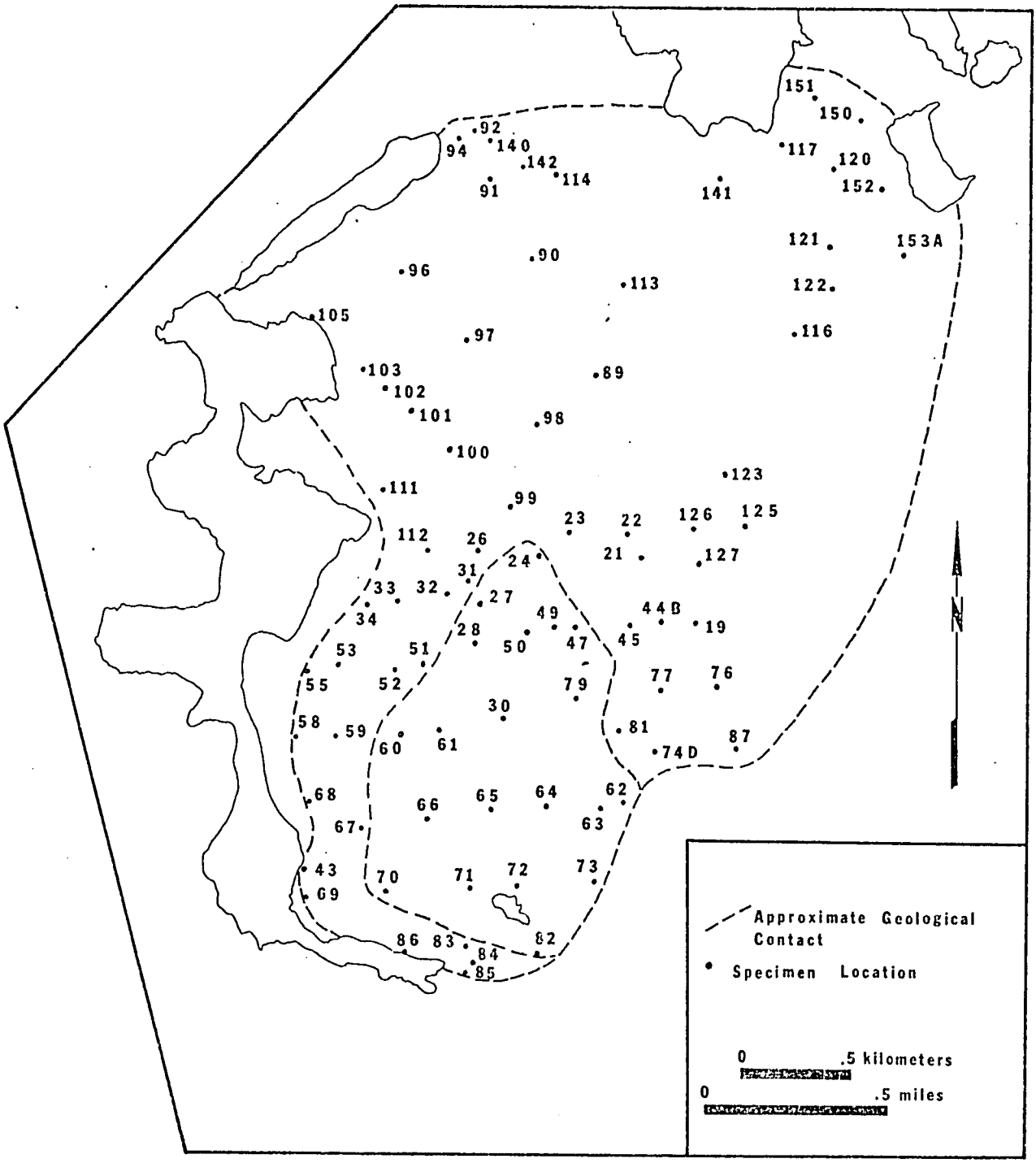

Figure 5 Locations of specimens of syenites I and II

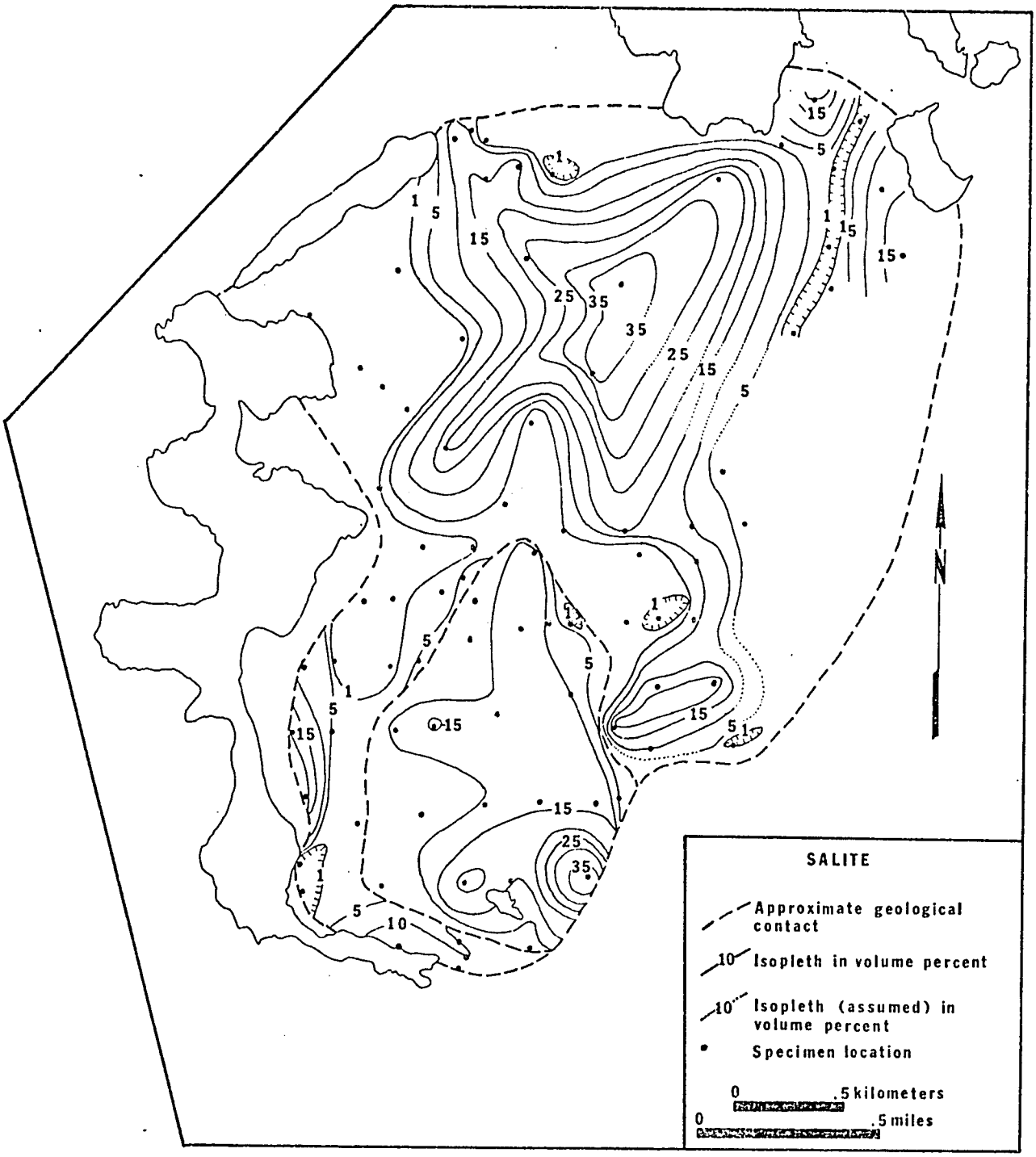

Figure 6 Isopleth map showing the distribution of salite in syenites I and II.

Barkevikite

Concentrations of barkevikite are high in the central part of syenite I, and gradually decrease toward the borders of the intrusion, where they are absent or present in trace amounts (Figure 7). However, in the marginal rocks of the northeastern and southern parts of the body, high concentrations of barkevikite are present (Figure 7).

Barkevikite is present in relatively high concentrations in the marginal rocks of syenite II, but only as trace amounts in rocks in the central part of the intrusion (Figure 7).

Biotite

The distribution pattern of biotite in syenite I is more complex than the patterns of salite and barkevikite. In addition to having a high concentration of biotite in the central part of the body, there are several areas in the northern part of syenite I, and between syenite II and the borders of syenite I, where there are high concentrations of biotite (Figure 8).

The distribution pattern of biotite in syenite II, consists of irregularly shaped areas of relatively high biotite concentrations in the northern and central parts of the intrusion, with several intervening troughs of low biotite concentrations (Figure 8).

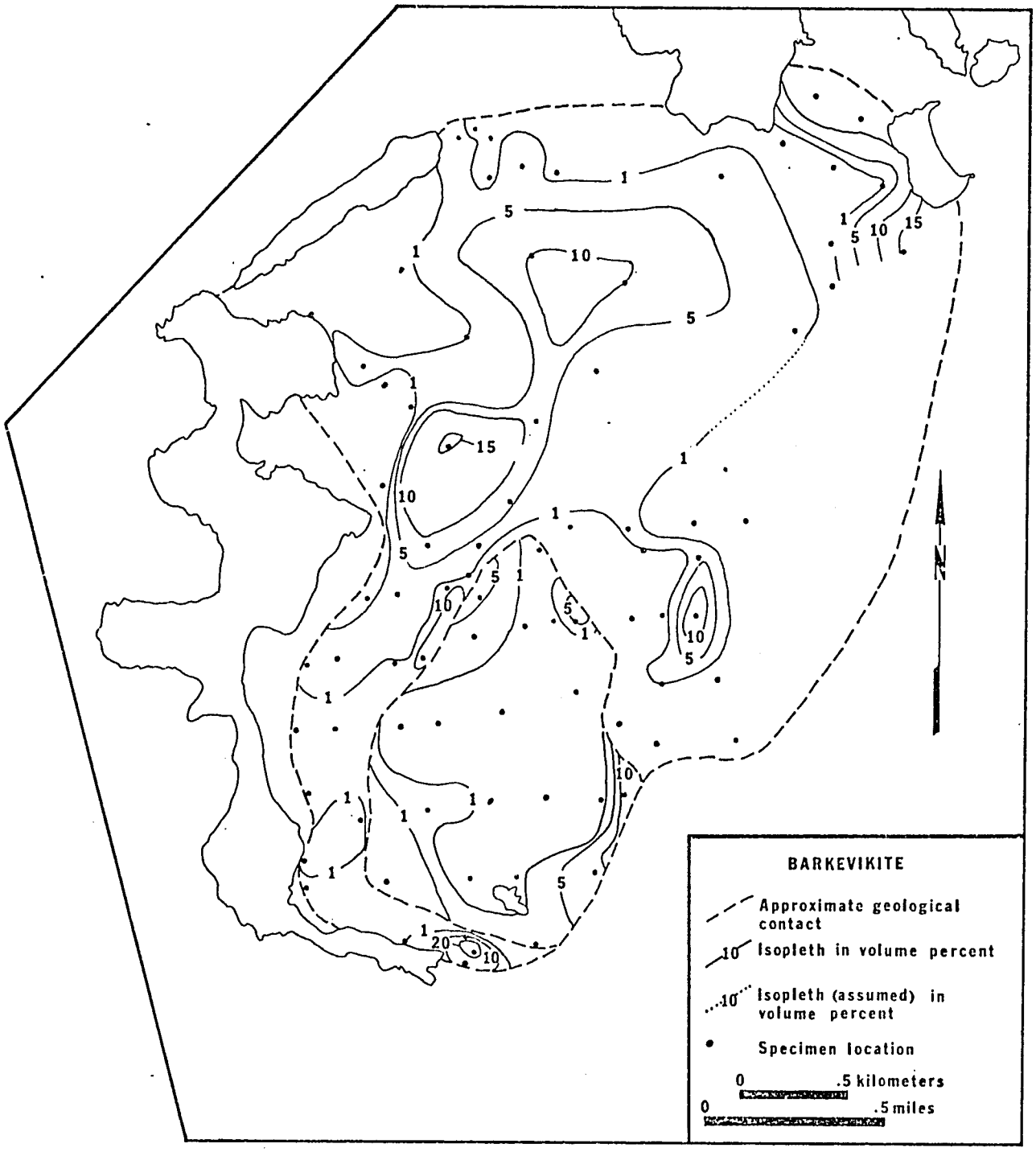

Figure 7 Isopleth map showing the distribution of barkevikite in syenites I and II.

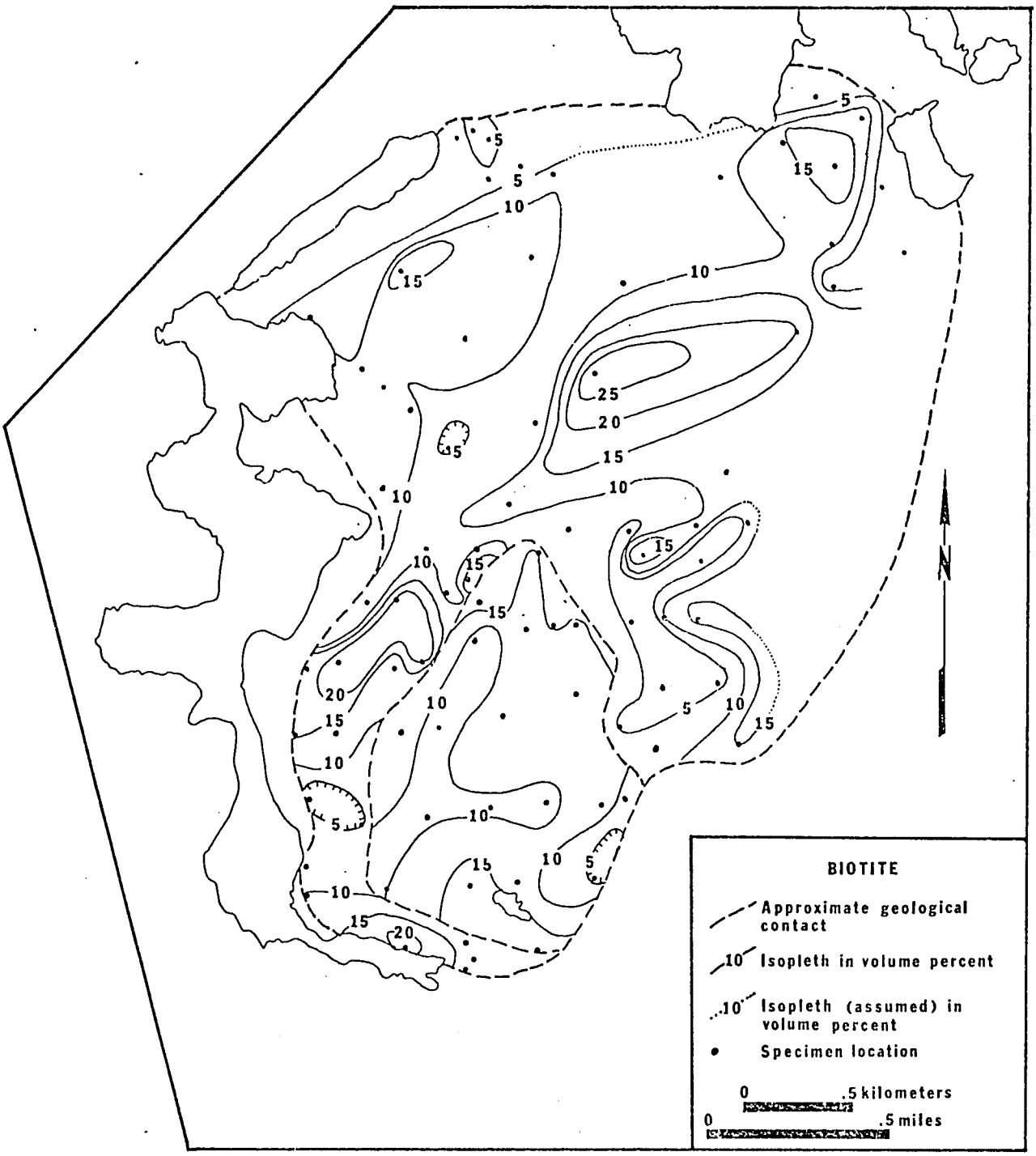

Figure 8 Isopleth map showing the distribution of biotite in syenites I and II.

Microperthite

In the north central part of syenite I, the proportions of microperthite are low and gradually increase toward the margins of the intrusion. These marginal highs, extend southward on both sides of syenite II, and form narrow irregular zones, in which the proportions of microperthite are high (Figure 9). However, in the northeastern, southwestern, and southern parts of syenite I, the marginal rocks have low proportions of microperthite (Figure 9).

The proportions of microperthite in syenite II are generally lower, but there are irregular shaped areas in the northeast and southwest parts of the intrusion, in which the proportions of microperthite are high (Figure 9).

Ore minerals (magnetite and ilmenite)

The concentrations of ore minerals are highest in the central part of syenite I and progressively decrease toward the borders of the intrusion. In addition, there are several small areas in the eastern, western and southern parts of syenite I where there are high concentrations of ore minerals (Figure 10).

The ore mineral content of syenite II is generally higher than that of syenite I, with the highest concentrations over large areas in the southern and northern parts of the intrusion (Figure 10).

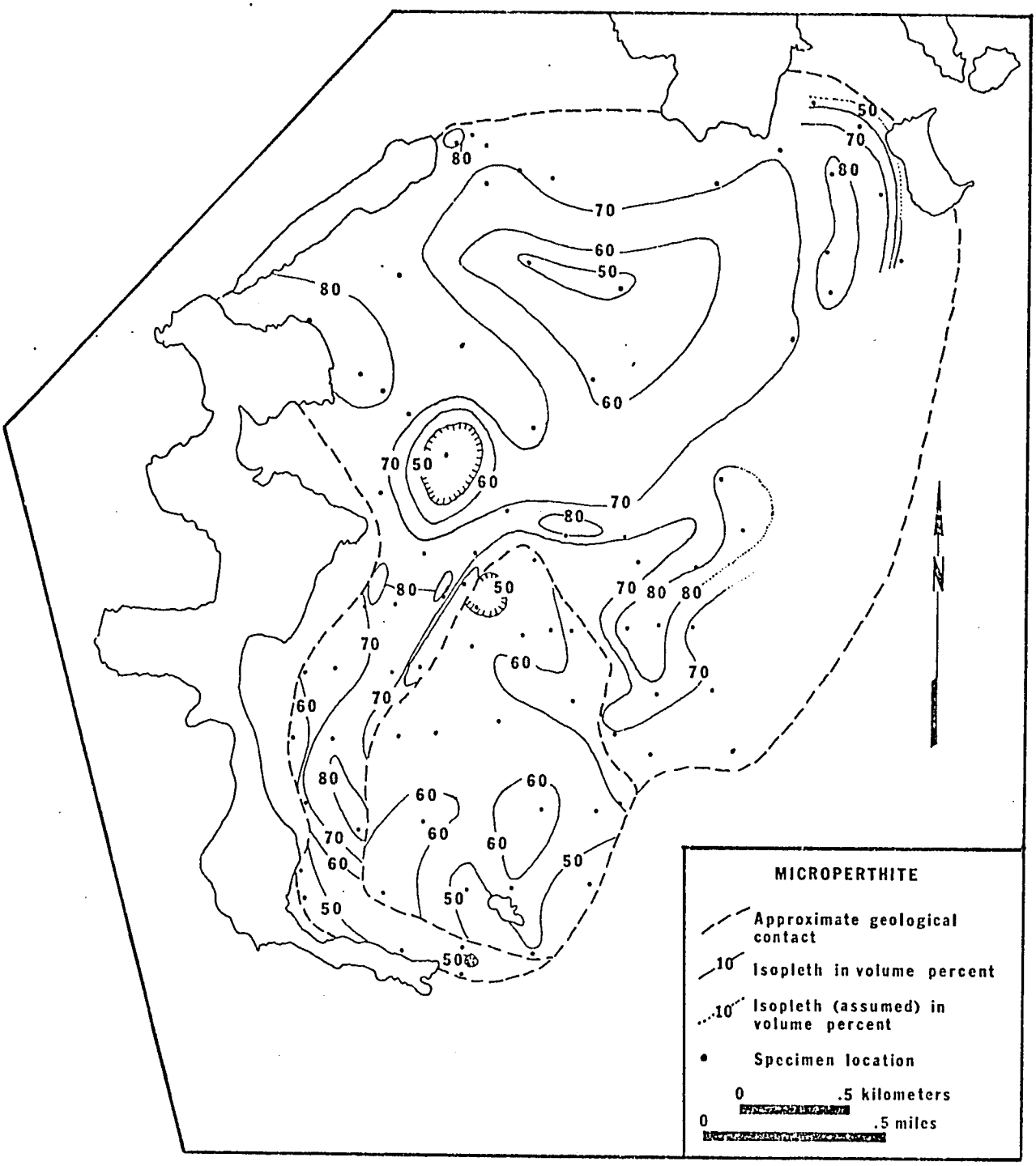

Figure 9 Isopleth map showing the distribution of microperthite in syenites I and II.

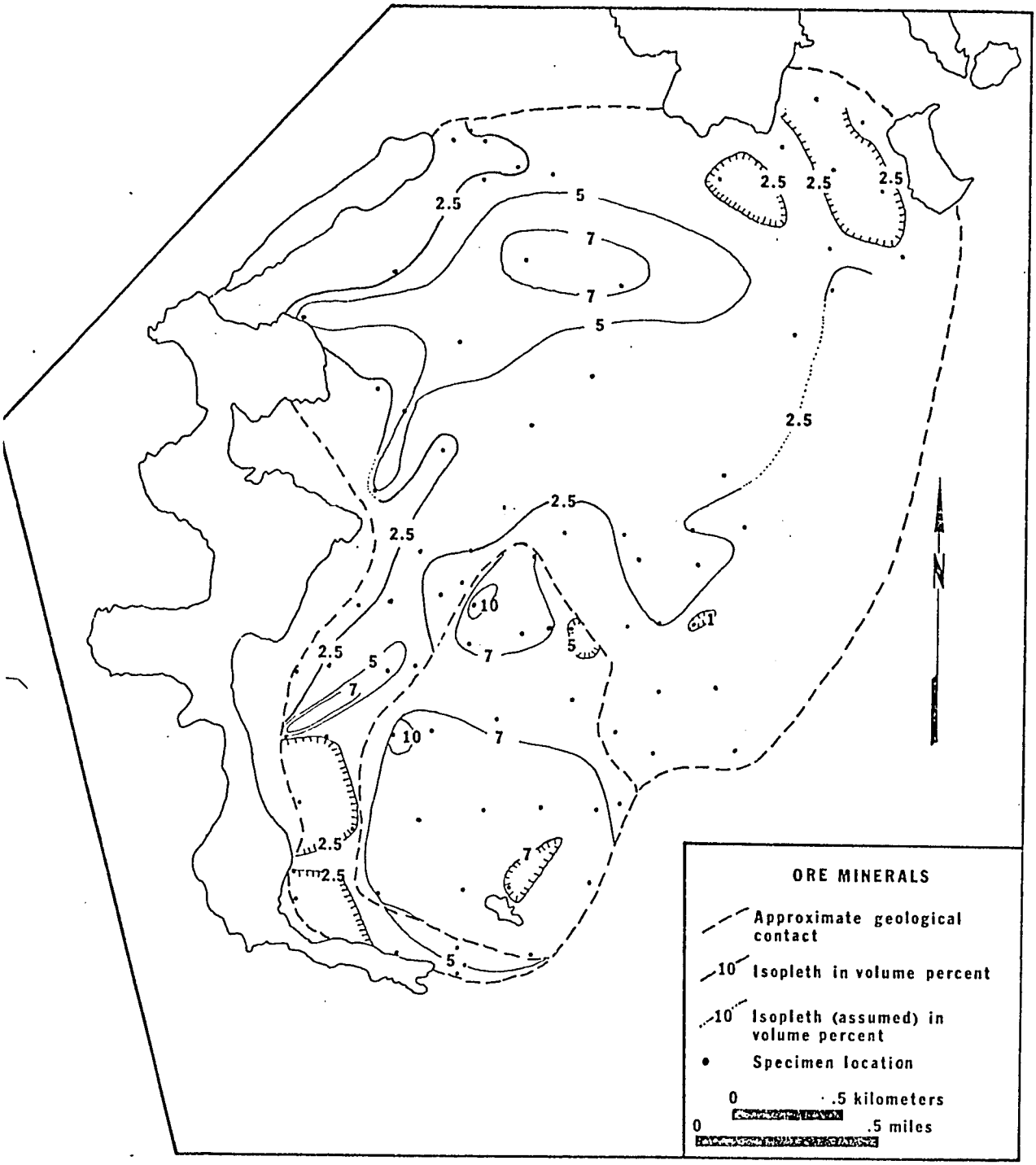

Figure 10 Isopleth map showing the distribution of ore minerals in syenites I and II.

Apatite

The proportions of apatite are high over a large irregularly shaped area in the central part of syenite I and gradually taper off toward the borders of the intrusion. However, close to the contact with syenite II, and along the borders of syenite I, there are several areas where these rocks contain high proportions of apatite (Figure 11).

The proportions of apatite in syenite II, are moderately high over most of the intrusion, and there are several small isolated areas, most of them near the margins of syenite II, where the rocks contain high proportions of apatite (Figure 11).

Calcite

The distribution pattern of calcite in syenite I is irregular and complex. In the northern part of the intrusion, there are two irregularly shaped areas of relatively high calcite concentrations which grade laterally into a trough of relatively low calcite concentration between the two, and into rocks near the margins of the intrusion which contain minor amounts of calcite (Figure 12). Immediately north of syenite II, the trough of low calcite concentration bifurcates and extends southwards on both sides of syenite II. The southward extensions of this trough enclose small areas which have relatively high concentrations of calcite (Figure 12).

In syenite II, calcite is present in minor amounts (<1%)

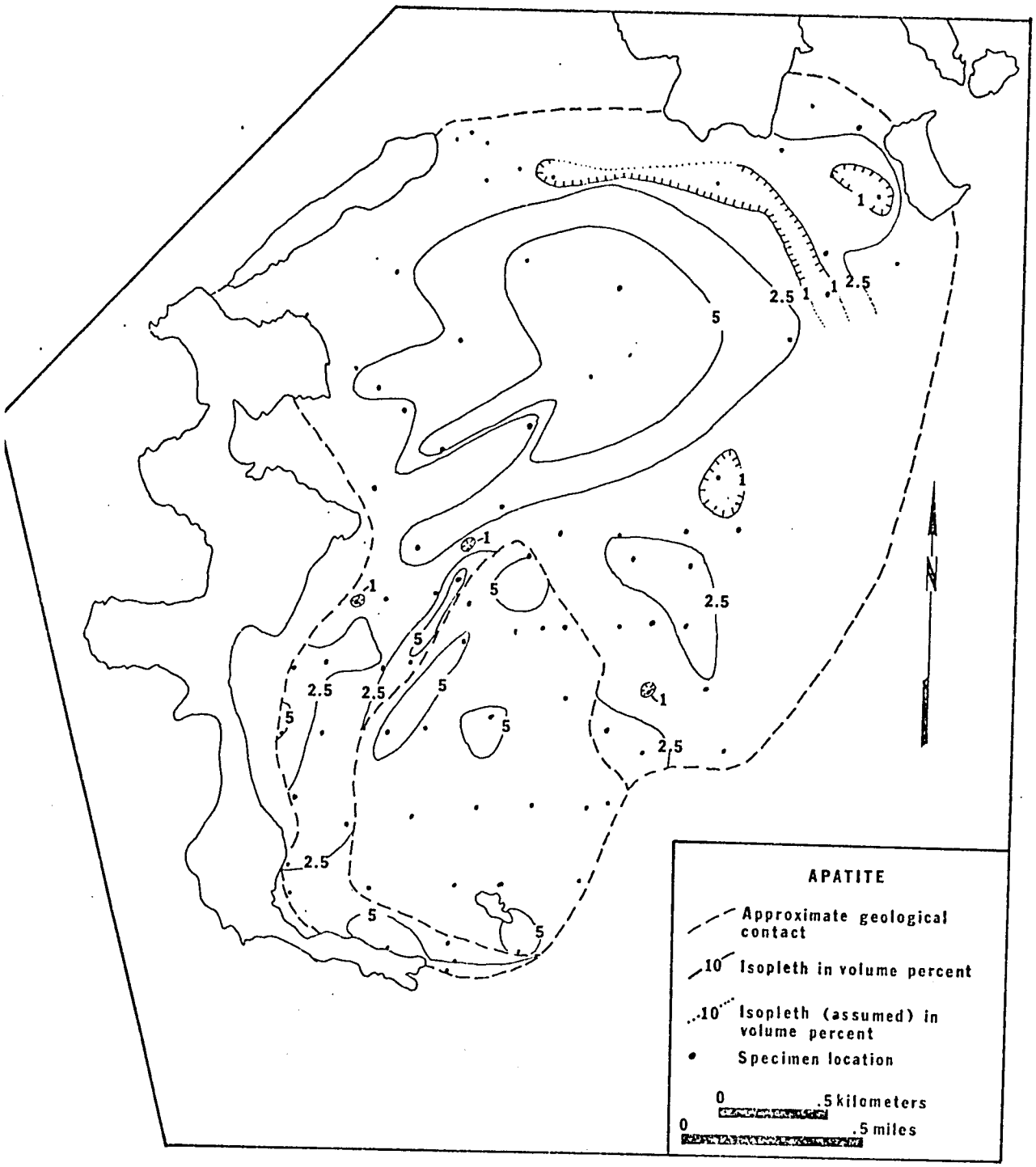

Figure 11 Isopleth map showing the distribution of apatite in syenites I and II.

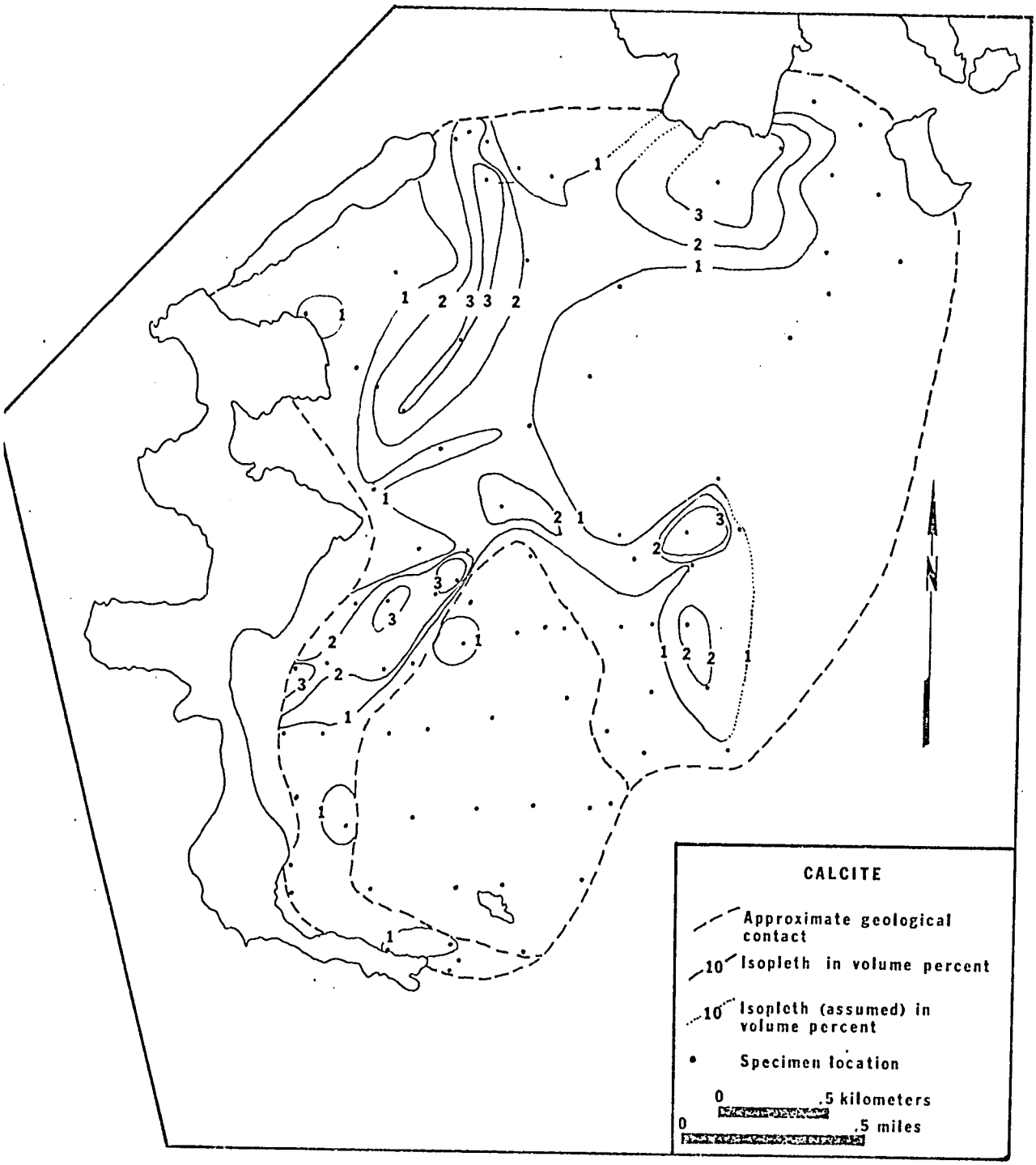

Figure 12 Isopleth map showing the distribution of calcite in syenites I and II.

over most of the intrusive. However, in the northwestern part of the intrusive, specimens MD-91, MD-97, and MD-101 contain somewhat greater amounts (3%) (Figure 12).

Other minerals

Plagioclase occurs throughout the rocks of syenites I and II as small relicts in microperthite crystals. In syenite II, and in the marginal rocks of syenite I, they constitute up to 10% of the mode. It also occurs as small rims around nepheline grains.

Nepheline occurs in only two localities (Figure 3), where it makes up 11-21% of the mode.

Sphene and epidote are present in minor amounts in syenites I and II and do not appear to have any regular distribution pattern.

CHAPTER V

CHEMISTRY OF SYENITES I AND II

Eleven specimens from syenites I and II were analysed for major elements. In syenite I, specimens were chosen so as to provide an east-west section across the body, whereas in syenite II, the specimens were chosen so as to provide both, east-west, and north-south sections across the intrusion (Figure 13).

These analyses along with their norms are presented in Tables VIII and IX. A comparison of the average compositions of the two syenites shows that in syenite I, the percentages of TiO_2, Fe_2O_3, FeO, MgO, CaO, P_2O_5, and L.O.I. are lower, and the percentages of SiO_2, Al_2O_3, K_2O, Na_2O, and CO_2 are generally higher than those in syenite II.

The oxide contents of syenites I and II, are shown in Figures 14 and 15. Examination of Figure 14 reveals that in syenite I, the Fe_2O_3, FeO, MgO, CaO, and P_2O_5 contents are low at the margins of the body, and increase toward the central part of the intrusion; and vice versa for the SiO_2, Al_2O_3, K_2O, and Na_2O contents. The TiO_2 content does not show any systematic variation across the body.

A study of Figure 15 shows that in syenite II, along the north-south section, the SiO_2, Al_2O_3, K_2O, and Na_2O contents

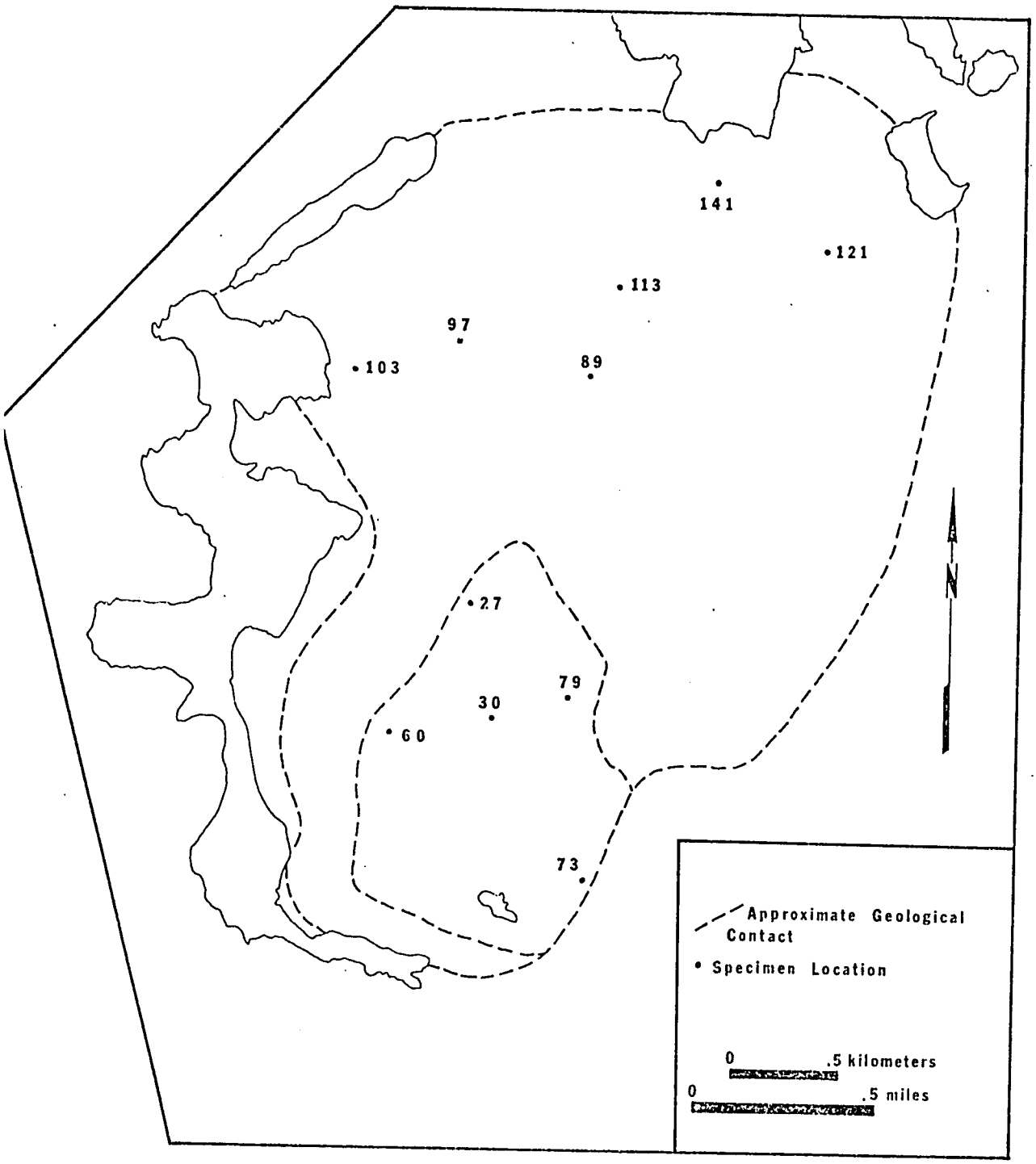

Figure 13 Map showing the location of specimens from syenites I and II which were selected for chemical analyses.

TABLE VIII

CHEMICAL COMPOSITION OF ROCKS FROM SYENITE I

specimen	103	97	89	113	141	121	average	%error of amount present
oxides	%oxides	%oxides	%oxides	%oxides	%oxides	%oxides	%oxides	
SiO_2	49.47	52.85	47.63	40.70	55.59	49.24	49.24	± 2
TiO_2	0.12	0.50	0.16	0.38	0.03	0.34	0.25	± 5
Al_2O_3	23.56	22.12	17.13	16.53	16.24	24.68	21.58	± 5
Fe_2O_3	3.61	3.43	2.92	9.59	2.59	2.34	4.08	± 5
FeO	1.62	2.00	3.52	4.54	1.59	1.37	2.44	± 2
MgO	1.76	2.72	5.26	4.90	2.06	1.39	2.84	± 2
CaO	2.31	2.16	9.29	10.64	12.01	2.63	7.18	± 3
K_2O	8.65	6.50	6.46	5.61	6.40	8.02	6.93	± 4
Na_2O	5.73	4.90	3.75	2.73	2.80	5.92	4.26	± 10
P_2O_5	0.97	1.18	3.75	3.01	0.00	0.97	1.64	
L.O.I.	1.01	1.13	1.26	0.58	0.21	1.09	0.88	
CO_2	0.00	1.40	0.00	0.48	1.73	0.30	0.65	
total	98.81	100.89	100.13	99.69	101.25	100.92	101.97	
Fe_2O_3/FeO	2.20	1.70	0.82	2.10	1.69	1.70	1.67	
FeO/MgO	0.94	0.73	0.66	0.92	0.77	0.98	0.85	
			NORMS (wt%)					
Corundum	2.89	7.02	-----	-----	-----	4.50	-----	
Orthoclase	51.12	38.41	38.17	33.15	37.82	47.39	40.95	
Albite	3.78	35.88	5.87	0.76	20.76	8.62	7.34	
Anorthite	5.12	-----	10.83	16.28	12.84	4.81	19.19	
Leucite	-----	-----	-----	-----	-----	-----	-----	
Nepheline	24.22	3.02	14.01	12.10	1.59	22.47	15.55	
Hematite	0.17	-----	-----	0.26	-----	-----	-----	
Wollastonite	-----	-----	4.49	3.75	6.13	-----	0.63	
Enstatite	-----	-----	3.18	3.24	5.13	-----	0.50	
Ferrosilite	-----	-----	0.92	-----	0.22	-----	0.05	
Forsterite	3.07	4.75	6.95	6.28	-----	2.43	4.60	
Fayalite	-----	0.01	2.21	-----	-----	0.02	0.50	
Magnetite	4.87	4.97	4.23	13.53	3.76	3.39	5.92	
Ilmenite	0.23	0.95	0.30	0.72	0.65	0.65	0.47	
Apatite	2.30	2.80	8.88	8.88	0.50	2.30	3.88	
Calcite	-----	1.08	-----	1.09	3.93	0.68	1.48	
total	97.85	98.90	100.05	100.04	101.57	97.25	101.17	

TABLE IX

CHEMICAL COMPOSITION OF ROCKS FROM SYENITE II

specimen	60	27	30	79	73	average	%error of amount present
oxides	%oxides	%oxides	%oxides	%oxides	%oxides	%oxides	
SiO_2	43.10	43.79	48.88	44.62	41.36	44.35	± 2
TiO_2	0.96	0.68	0.43	0.70	0.32	0.61	± 5
Al_2O_3	19.07	16.61	20.64	21.31	12.93	18.11	± 5
Fe_2O_3	5.57	9.43	4.98	5.60	9.83	7.08	± 5
FeO	4.41	6.10	3.55	3.61	6.08	4.75	± 2
MgO	3.71	2.68	3.40	3.28	5.18	3.65	± 2
CaO	8.14	8.86	8.12	7.49	14.35	9.39	± 3
K_2O	5.34	7.35	4.28	5.16	4.38	5.30	± 4
Na_2O	4.49	2.57	3.46	3.93	2.49	3.30	± 10
P_2O_5	2.36	1.77	2.19	1.61	1.89	1.96	
L.O.I.	2.39	0.89	1.25	1.55	2.21	1.65	
CO_2	0.00	0.00	0.00	0.00	0.00	0.00	
total	99.54	100.73	100.89	98.86	100.99	100.23	
Fe_2O_3/FeO	1.26	1.54	1.40	1.55	1.61	1.44	
FeO/MgO	1.18	2.27	1.04	1.10	1.17	1.30	
			NORMS(wt%)				
Corundum	-----	-----	0.80	-----	-----	-----	
Orthoclase	31.56	26.59	25.29	30.49	6.35	31.32	
Albite	2.03	-----	25.43	7.11	-----	3.35	
Anorthite	16.11	12.08	25.98	25.27	11.17	18.95	
Leucite	-----	13.21	-----	-----	15.31	-----	
Nepheline	19.48	11.78	2.09	14.16	11.41	13.31	
Hematite	-----	-----	-----	-----	-----	-----	
Wollastonite	3.70	8.48	-----	0.57	19.90	6.19	
Enstatite	2.76	5.81	-----	0.46	12.90	4.63	
Ferrosilite	0.57	1.99	-----	0.05	2.52	0.95	
Forsterite	4.54	0.60	5.93	5.40	-----	3.13	
Fayalite	1.03	0.23	1.31	0.62	-----	0.71	
Magnetite	8.08	13.67	7.22	8.12	14.25	10.27	
Ilmenite	1.82	1.29	0.82	1.33	0.61	1.16	
Apatite	5.59	4.19	5.19	3.81	4.48	4.64	
Calcite	-----	-----	-----	-----	-----	-----	
total	97.27	99.93	100.04	97.39	98.91	98.60	

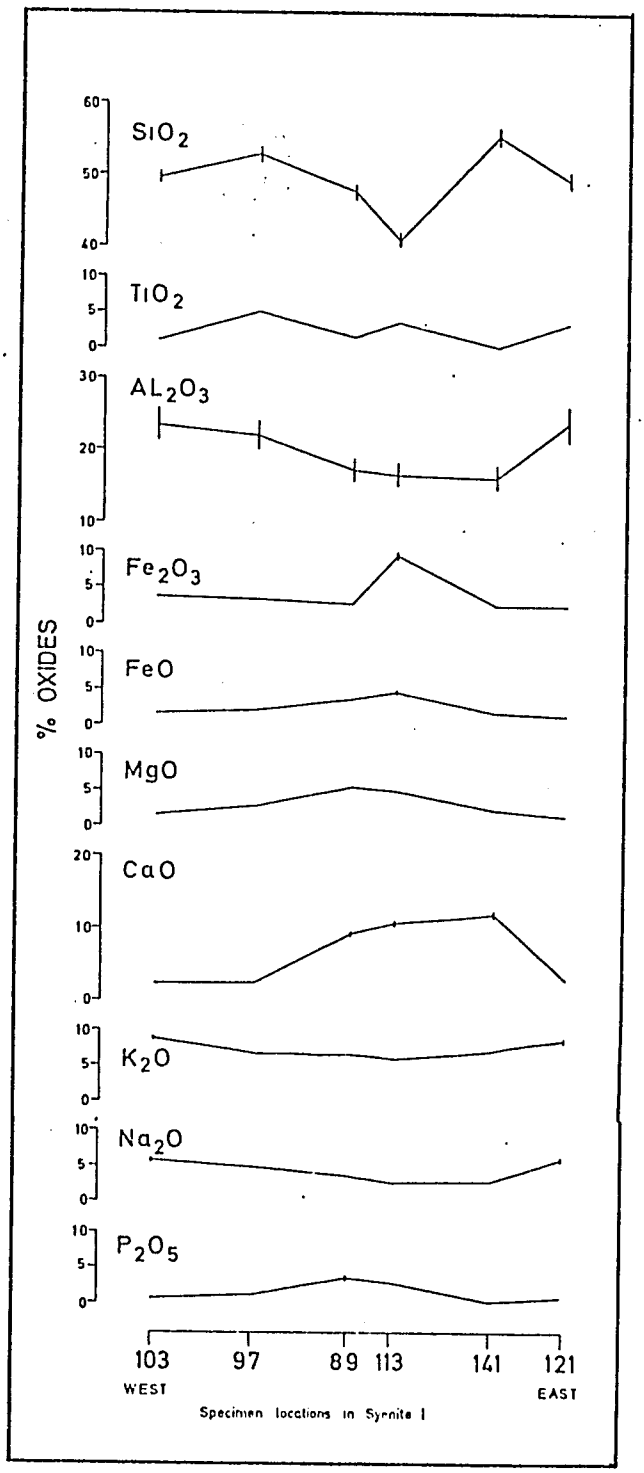

Figure 14 Diagram showing the variations in oxide content in syenite I

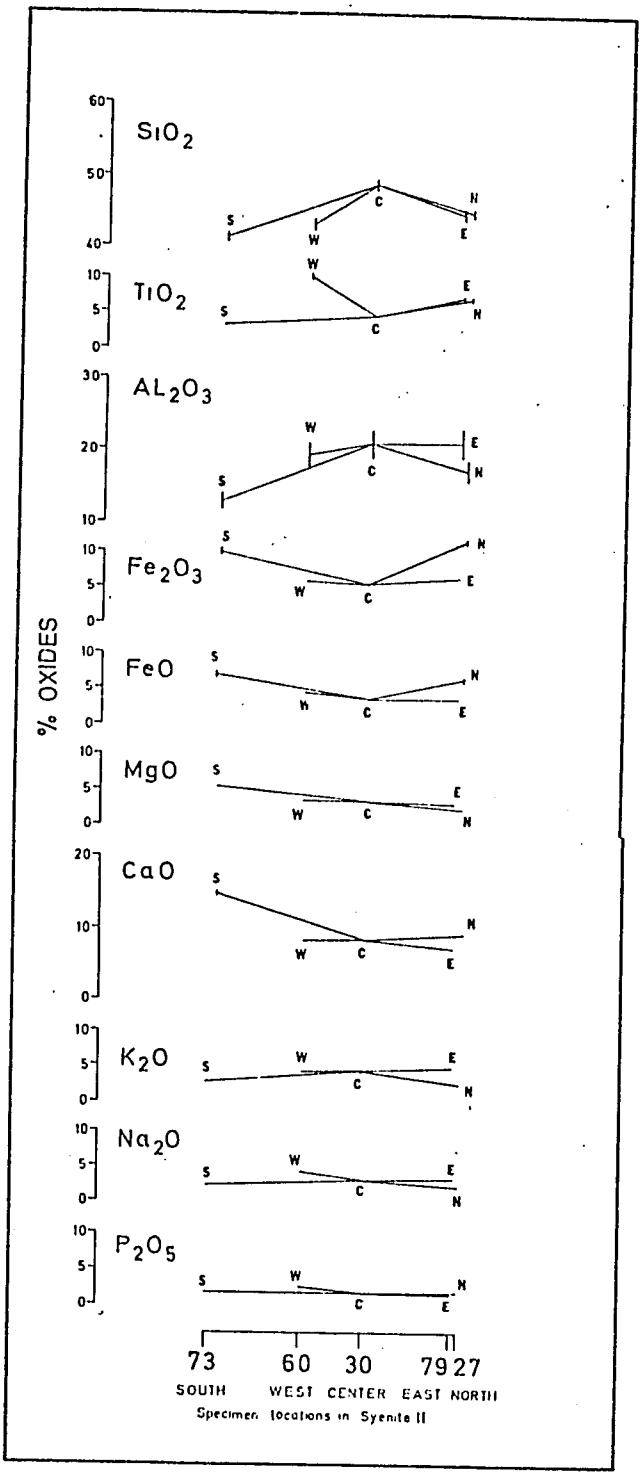

Figure 15 Diagram showing the variations in oxide content in syenite II.

are low in the marginal rocks, and increase toward the center of the intrusion. The opposite is true for the Fe_2O_3, FeO, and CaO contents. The TiO_2 content is low in the southern part of the intrusion and gradually increases northward; and vice versa for the MgO content. The P_2O_5 content does not vary along this section.

Along the east-west section the Fe_2O_3, FeO, MgO, CaO, K_2O, Na_2O, and P_2O_5 contents do not show any significant variations. For SiO_2, and Al_2O_3, the pattern is similar to that along the north-south section. The TiO_2 is low in the central part of syenite II, and increases toward the margins.

A comparison of Figures 14 and 15 reveals that the rocks of syenites I and II, are differentiated along opposite trends. The explanation for these opposing trends lies in the fact that in syenite II, the pyroxene-rich rock (Plate 5) is not centrally located as in syenite I (see location of specimen 73, Figure 13). If in Figure 15 the location of specimens 30 and 73 were interchanged, the differentiation trends would be similar to those in syenite I.

CHAPTER VI

DISCUSSION

Estimates of temperature, fO_2, fH_2O, and $aSiO_2$ during the crystallization of syenites I and II

Petrographic examination of specimens from syenite I reveals that there are several assemblages which are favorable for determining the temperature, the oxygen and water fugacities, and the silica activities at the time of crystallization.

Several grains of nepheline and microperthite in contact with each other, from specimen MD-84A(Table V), were analysed using an electron microprobe. Using the geothermometer proposed by Perchuk and Ryabchikov (1968), this assemblage yields temperatures of crystallization of approximately 750°-$800^{\circ}C$.

This geothermometer was refined by Powell and Powell (1975). Using the refined method, this assemblage yields temperatures of crystallization of approximately $730^{\circ}C$. Temperatures obtained using the latter method are probably more accurate because values of excess silica are taken into consideration. As will be seen in a subsequent section, nepheline does not appear to have crystallized very early in the crystallization sequence. Therefore it is probable that the temperature of the magma was somewhat higher than $730^{\circ}C$ at the time of intrusion.

Several grains of magnetite and ilmenite were analysed in order to determine the oxygen fugacity, and temperature of crystallization, using the method proposed by Buddington and Lindsley(1964). Since the magnetite contains only trace amounts of TiO_2, and the ilmenite is not of the ferrian type, these parameters could not be determined using this method.

Wones and Eugster (1965) in their study on the stability of biotite, derived an expression relating the fugacity of water, the fugacity of oxygen, temperature of crystallization, and mole fraction of annite in biotite, in assemblages containing magnetite, biotite, and sanidine. This expression was modified by Wones (1972). The modified expression is as follows:

$$\text{Log } fH_2O = 7409/T + 4.25 + 1/2 \log fO_2 + 3\log X - \log a^{\text{feldspar}}_{KAlSi_3O_8} - \log a^{\text{magnetite}}_{Fe_3O_4}$$

where, X equals the Fe^{+2}/Fe^{+2}+ Mg ratio in biotite, fH_2O equals the fugacity of water, fO_2 equals the fugacity of oxygen, $a^{\text{feldspar}}_{KAlSi_3O_8}$ equals the activity of K-feldspar in feldspar, $a^{\text{magnetite}}_{Fe_3O_4}$ equals the activity of Fe_3O_4 in magnetite, and T equals absolute temperature.

This assemblage is present in specimen MD-84A, and throughout most of syenite I. The activity of $KAlSi_3O_8$ in the microperthite was calculated from the microprobe analysis (see Table V) using the activity coefficients of Luth, Fenn,

and Martin (1970).

The magnetite in specimen MD-84A contains less than 1 mole % ulvospinel component. Since the magnetite occurs as discreet grains, and not as intergrowths with ilmenite or sphene, it is unlikely that it initially contained appreciably more titanium. Accordingly, the activity of pure magnetite (1.0) was used in the calculations.

Since data on the Fe^{+3} content in biotite from this specimen is not available , a number of values (0.7 and 0.6) were assumed for the Fe^{+2}/Fe^{+2} + Mg ratio. The first value was calculated from the biotite analysis in Table IV: assuming that there is no ferric iron in the biotite. The second ratio was calculated assuming that there is approximately 2 percent Fe^{+3} in the biotite. Nash and Wilkinson (1970) in their study of similar rocks, reported similar values of Fe^{+3} in biotite. It is also assumed that there is no fluorine in the biotite.

A range of values (-14.6 to -17.4) for log fO_2 were obtained by using the temperature of 730°C, from the nepheline-feldspar geothermometer, and using it in conjunction with Figure 4, p 315, of Buddington and Lindsley (1964).

The results of these calculations are shown in Table X.

TABLE X

ESTIMATES OF WATER FUGACITY DURING THE CRYSTALLIZATION OF SYENITE I

Temperature °C	Log O_2 fugacity	$X=Fe^{+2}/Fe^{+2}+Mg$	$aKAlSi_3O_8$	aFe_3O_4	Fugacity of water(bars)
730	-14.6	0.70	0.79	1.0	9772
730	-14.6	0.60	0.79	1.0	6025
730	-15.0	0.70	0.79	1.0	6165
730	-15.0	0.60	0.79	1.0	3801
730	-16.0	0.70	0.79	1.0	1950
730	-16.0	0.60	0.79	1.0	1202
730	-16.5	0.70	0.79	1.0	1096
730	-16.5	0.60	0.79	1.0	676
730	-17.0	0.70	0.79	1.0	490
730	-17.0	0.60	0.79	1.0	302
730	-17.4	0.70	0.79	1.0	389
730	-17.4	0.60	0.79	1.0	240

Examination of this table shows that there is a large range in fH_2O values. Buddington and Lindsley (1964), Morse (1967), Nash and Wilkinson (1970) in their studies of syenitic rocks, determined that the oxygen fugacity was very close to that of the QFM buffer during crystallization.

At 730°C, the value of the log fO_2 on the QFM buffer is -16.5. Assuming that the oxygen fugacity was close to that of the QFM buffer, then values of log fH_2O calculated using values of log fO_2 greater than -16 and less than -17 can be discarded. This narrows down the range of fH_2O from 302 to 1950 bars.

The presence of calcite as a late primary phase in syenite I is indicative of a fairly high CO_2 fugacity. This in turn suggests that the total pressure was probably considerably greater than the fugacity of water, probably in the kilobars range. It also suggests that the fH_2O:fCO_2 ratio decreased with time. The absence of chilled margins, and contact metamorphic effects, also suggests that syenite I was emplaced at appreciable depths in the crust.

The silica activity in the nepheline-bearing syenite at the time of crystallization is defined by the following reaction:

$$1/2 \text{ Nepheline} + SiO_2^{glass} = 1/2 \text{ high Albite}$$

For this expression we can use the following:

$\text{Log } aSiO_2 = Gr^o/2.303(RT) + 1/2 \log a^{\text{Perthite}}_{\text{Albite}} - 1/2 \log a^{\text{Nepheline}}_{NaAlSiO_4}$

where, $aSiO_2$ equals the activity of silica, Gr^o equals the free energy change of the standard state reaction, $a^{\text{Perthite}}_{\text{Albite}}$ equals the activity of albite in perthite, $a^{\text{Nepheline}}_{NaAlSiO_4}$ equals the activity of $NaAlSiO_4$ in nepheline, and T equals the absolute temperature.

Substituting the appropriate values in the above expression

$\text{Log } aSiO_2 = -3988/2.303(1.9872)(730+273) + 1/2 \log 0.7 - \log 0.73$

$\text{Log } aSiO_2 = -0.88$

This value is slightly lower than that of the albite-nepheline buffer at the same temperature.

Data for the standard state reaction was obtained from Robie and Waldbaum (1968). The activity of albite in the microperthite was calculated from a microprobe analysis (see Table V, specimen MD-84A) using the activity coefficients of Luth, Fenn, and Martin (1970). The activity of $NaAlSiO_4$ in the nepheline was calculated from microprobe analyses (see Table VI). Values for the temperature were obtained from the nepheline - feldspar geothermometer.

According to Carmichael *et al*,(1974, pp 274-275), the amount of aluminium and titanium in pyroxene is dependent on the silica activity in the melt; the lower the silica activity in the melt, the higher the aluminium and titanium contents in the pyroxene. The high aluminium and titanium contents in

salites from syenite I, indicate that the silica activity in the melt at the time of salite crystallization was low. Likewise, the presence of nepheline indicates that the silica activity was low, at the time of nepheline crystallization. As will be seen in a subsequent section, salite and nepheline appear to have crystallized as early and late phases respectively. This suggests that the silica activity in the melt was low throughout the crystallization history of syenite I.

However, the presence of a quartz syenite dyke on the western shore of Castor Blanc Lake (Figure 3), argues against this hypothesis. A possible explanation for this contradiction, is that the syenite dyke in question, has been contaminated by the assimilation of siliceous rocks. An alternate possibility, is that a quartz-bearing phase was present in the uppermost part of the magma chamber, and has since been removed by erosion. The author prefers the first possibility.

The absence of nepheline in syenite II precludes the use of the nepheline - feldspar geothermometer for this phase of the pluton. However, due to the close textural and mineralogical similarities between syenites I and II, it is highly probable that its temperature at the time of intrusion was similar to that of syenite I. The oxygen and water fugacities were probably also in the same range as in syenite I.

Crystallization history of syenite I

The ore minerals in syenite I occur as very small inclusions in the other minerals which make up syenite I, and as irregular shaped interstitial grains (Plates 4,7,10, and 19). The latter mode of occurrence accounts for most of the magnetite in syenite I. This suggests that most of the magnetite crystallized fairly late in the crystallization history of syenite I. Additional evidence in support of this hypothesis, lies in the fact that the magnetite in syenite I has very low titanium contents(see Table VII). If during the crystallization of syenite I, the oxygen fugacity was close to that of the QFM buffer; magnetite could not have crystallized early at high temperatures.

Since ilmenite and magnetite occur as discreet grains, the paragenetic relationship between the two minerals is not known. The fact, that ilmenite occurs mainly as an interstitial mineral, suggests that it also may have crystallized fairly late in the crystallization history of syenite I. However, it is also possible that it crystallized fairly early, and that with advancing crystallization was squeezed into the interstitial spaces between the other minerals.

The high concentrations of magnetite in the central part of syenite I, are probably due to concentration of iron in

the interstitial liquid. What caused it to crystallize late is a matter of conjecture: perhaps a change to more oxidizing conditions in the residual liquid. This could be accomplished by having the oxygen fugacity fall less rapidly with temperature toward the end of crystallization. This process also provides an explanation for the exsolved magnetite lamellae observed in salite.

Salite occurs as inclusions in microperthite, barkevikite, biotite, and ore minerals, in the central part of syenite I (Plates 4,10, and 19). These textures indicate that they crystallized prior to the minerals enclosing them. In the marginal rocks they occur as interstitial grains (Plate 6). This suggests, that they crystallized later than the associated rock-forming minerals and probably later than salite in the central part of the intrusive.

The FeO/MgO ratios in salite from syenite I lend additional support to this hypothesis. This ratio is higher in salites in the marginal rocks, than in salites in rocks from the central part of the intrusive (see Table II). This could be achieved by the early crystallization of large amounts of Mg-rich salite, thereby increasing the Fe/Mg ratio in the melt. Salite crystallizing at a later date would be richer in iron.

The high titanium and aluminium contents in all of the salites analysed, indicate that the silica activity in the

melt did not increase appreciably during the crystallization of salite.

Apatite occurs as inclusions in salite, ore minerals, barkevikite, biotite, and microperthite, and interstitially between these minerals (Plates 4,9,10, and 19). These textures indicate that apatite started crystallizing early, and continued to do so throughout much of the crystallization history of syenite I. However, as with ilmenite, it is possible that much of the interstitial apatite crystallized early, and was subsequently squeezed into interstitial spaces as a result of advancing crystallization.

The intimate association of salite and apatite in the central part of syenite I, suggests, that they crystallized at the same time. Also, the high concentrations of these minerals in the central part of the intrusive suggests that they were concentrated there by the same process or mechanism.

On the basis of textural evidence; crystallization of early, salite, apatite, and possibly ilmenite, appears to have been followed by the crystallization of the feldspars. Crystals of microperthite containing irregular patches of calcic oligoclase (Plate 14) are common throughout most of syenite I. Textures such as this suggests that plagioclase crystallized prior to the alkali feldspar; and was subse-

quently almost completely replaced by the alkali feldspar. This was followed by the exsolution of albitic plagioclase from the alkali feldspar at lower temperatures.

Inclusions of salite, apatite, and ore minerals in barkevikite, and biotite (Plates 4, 10, and 19), indicate that barkevikite and biotite formed later than these minerals. Reaction rims of barkevikite and biotite around salite grains (Plate 7) indicate that salite was no longer in equilibrium with the melt. They probably formed in response to increasing volatile content, increasing K_2O activity, and/or decreasing temperatures in the magma.

The Fe^{+2}/Fe^{+2} + Mg ratio of barkevikite and biotite in salite-bearing rocks reflects to a considerable degree that of the salite in the rocks (Figure 16A, specimens MD-113, and MD-22).* This is what would be expected if they were derived from the salite. In rocks in which there is no salite, the biotite composition reflects the composition of the residual magma, and is richer in iron (Figure 16A, specimen MD-84).

The absence of biotite or barkevikite rims around salite inclusions in microperthite (Plates 10 and 19), suggests that they started to crystallize later than the

* Figure 16 is not a true phase diagram or equilibrium diagram, but merely a compositional diagram. In addition, the dotted lines do not represent tie lines in the normal sense.

Projection point is K-feldspar

$$M = \frac{[MgO]}{[MgO] + [FeO]}$$

$$A = \frac{[Al_2O_3] - [K_2O]}{[Al_2O_3] - [K_2O] + [FeO] + [MgO]}$$

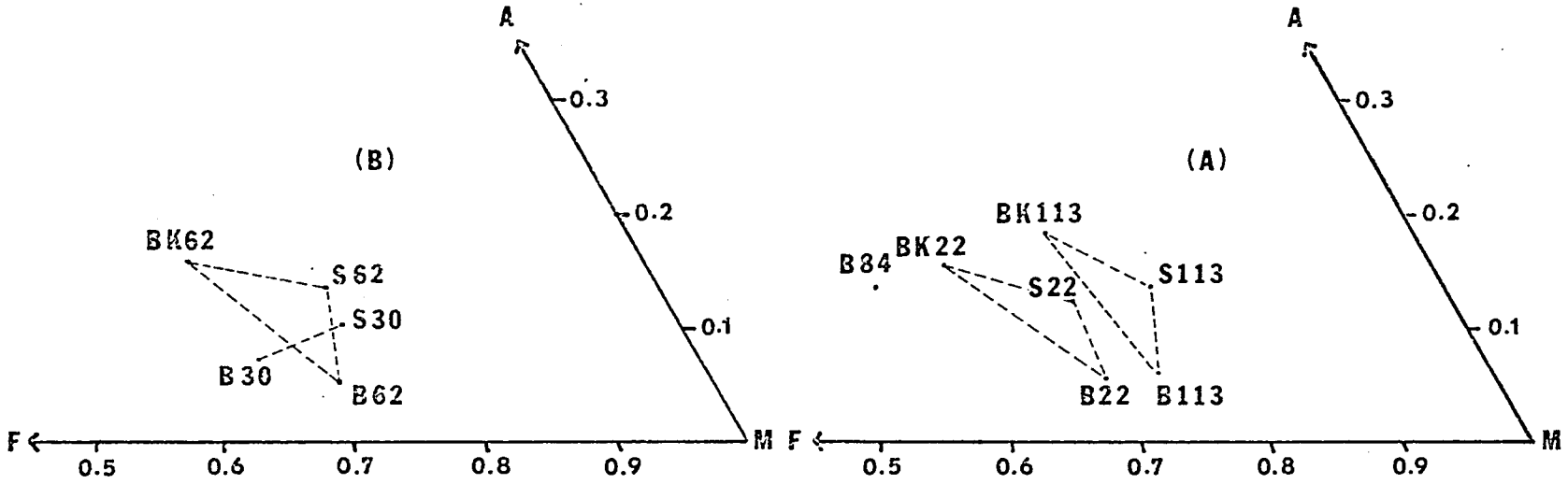

Figure 16 AFM diagram showing the relationships between salite(S), barkevikite(BK), and biotite(B) in syenites I and II.

microperthite. Textures in the marginal rocks of syenite I (Plate 11) suggest that biotite and barkevikite crystallized at the same time or later than the microperthite.

Nepheline was observed in rocks from two localities along the margins of syenite I (Figure 3). In these rocks nepheline occurs interstitially along with microperthite, biotite, and ore minerals, between much larger microperthite crystals (Plate 20). It also forms small inclusions in large microperthite grains (Plate 21). These textures indicate that nepheline crystallization extended over a time range.

It is suggested that crystallization of substantial amounts of salite, and alkali feldspar, prior to the crystallization of nepheline and alkali feldspar in the marginal rocks, is responsible for the low silica activity in the remaining magma. Nepheline probably formed in response to decreasing silica activity in the remaining magma.

Rims of albite were observed around nepheline inclusions in microperthite (Plate 21), but not around interstitial nepheline grains. This suggests that the early nepheline may have crystallized at high temperatures, and accomodated excess silica which was later exsolved as albite rims. Later nepheline may have crystallized at lower

temperatures and contained less excess silica in solution. It therefore retained its excess silica even at low temperatures (Hogarth 1976, personal communication).

Calcite occurs as irregular shaped interstitial crystals between the other minerals in syenite I. On this basis it is interpreted as a late stage primary mineral. It is unlikely that it is hydrothermal or deuteric in origin, as the surrounding minerals show no sign of hydrothermal or deuteric alteration. Its presence in these rocks is indicative of high CO_2 pressures during the late stages of crystallization.

The sequence of crystallization in syenite I outlined in the preceeding pages, is summarized graphically in Figure 17.

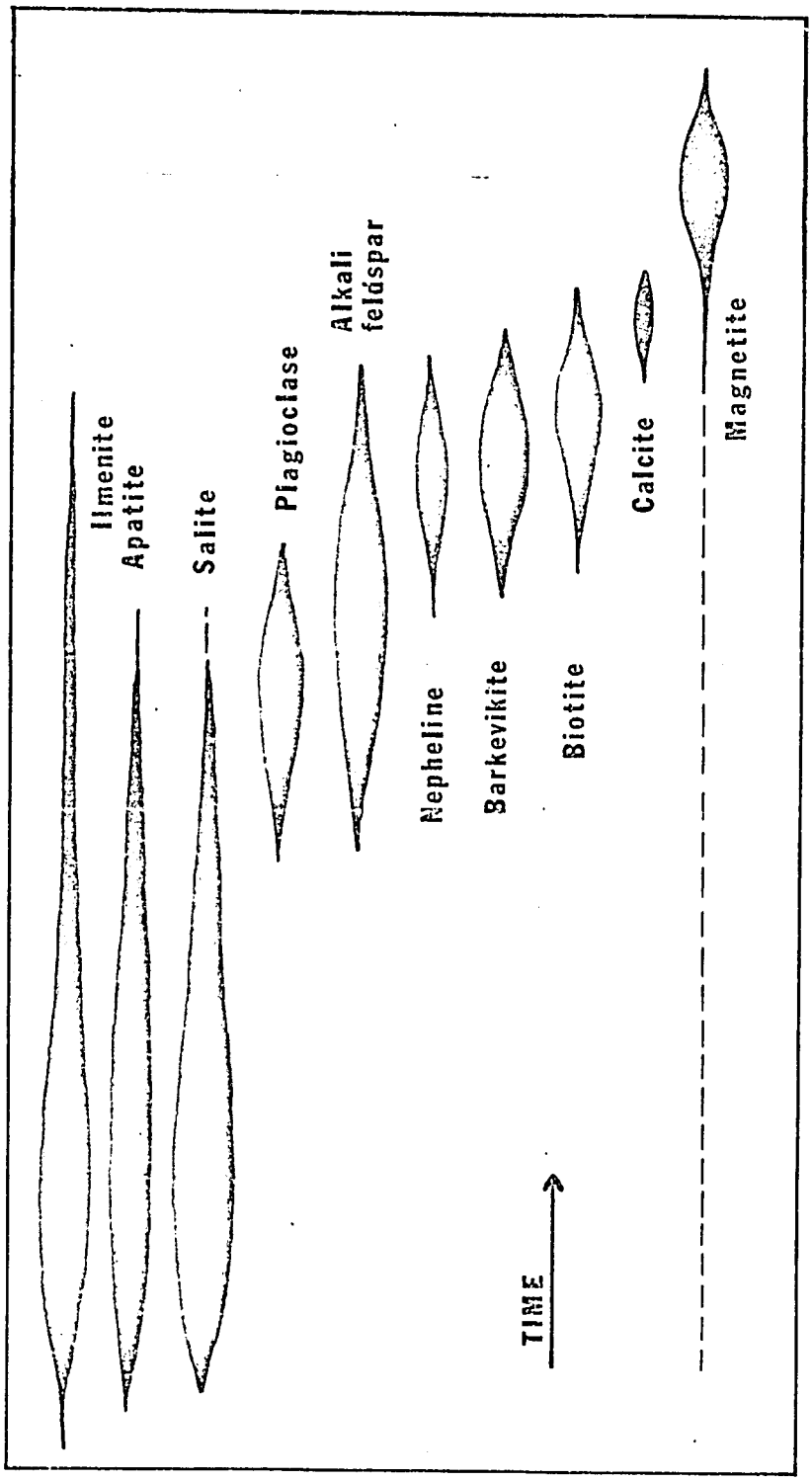

Figure 17 Schematic diagram showing the crystallization history of syenite I.

Crystallization history of syenite II

Syenites I and II appear to have had very similar crystallization histories. However, there are some differences in the crystallization histories of the two intrusives. Syenite II is considerably smaller than syenite I, and there are variations in grain size across the body. The rocks range from medium grained in the central part, to fine grained at the margins of the intrusive. This indicates that syenite II was intruded into relatively cold rocks, and probably cooled relatively quickly. Also, the rocks of syenite II contain numerous small cracks and fissures, which may be due to shrinkage during cooling and consolidation. The rocks of syenite I adjacent to syenite II, also contain numerous small cracks and fissures; which are possibly due to the forceful intrusion of syenite II.

The chemistry of biotite and barkevikite rims around salite grains refects the composition of the salite in the same manner as in syenite I (Figure 16B, specimen MD-62). Also plotted in Figure 16B, is the composition of one of the large biotite flakes (specimen MD-30) which occurs along cracks and fissures in syenite II, and in the rocks of syenite I near syenite II (Plates 12 and 13). As can be seen in Figure 16B, these large biotite flakes do not reflect the composition of the salite in the same rock. The higher iron content in these biotites suggests that they crystallized

later than those which occur as rims around salite and barkevikite grains. Their compositions probably reflect the composition of the late stage liquid. Their mode of occurrence also suggests that they crystallized very late in the crystallization history of syenite II; possibly along shrinkage cracks. Their presence in the rocks of syenite I, adjacent to syenite II, indicates that some of the volatiles escaped from the magma chamber along cracks and fissures.

The absence of calcite in most of syenite II, may be due to loss of CO_2 from the system along these cracks; or to initially low CO_2 fugacity. Escape of volatiles from the magma chamber also provides an explanation for the alteration of salite grains in the rocks of syenite I which are adjacent to syenite II (Plate 9).

Nepheline is also absent from syenite II.This is probably due to a relatively high silica activity in the melt throughout the crystallization history of syenite II. The high silica activity in the melt, is probably due to the fact that less alkali feldspar crystallized from the melt in syenite II, than in syenite I (Figure 9).

Another difference between syenites I and II, is that in syenite II, the replacement of plagioclase by alkali feldspar is not as complete as in syenite I. In syenite II,

the irregular plagioclase patches in alkali feldspar are larger than in syenite I (compare Plates 14, 18, and 15, 16, 17). This is probably due to the more rapid cooling and consolidation of syenite II.

The crystallization history of syenite II is summarized graphically in Figure 18.

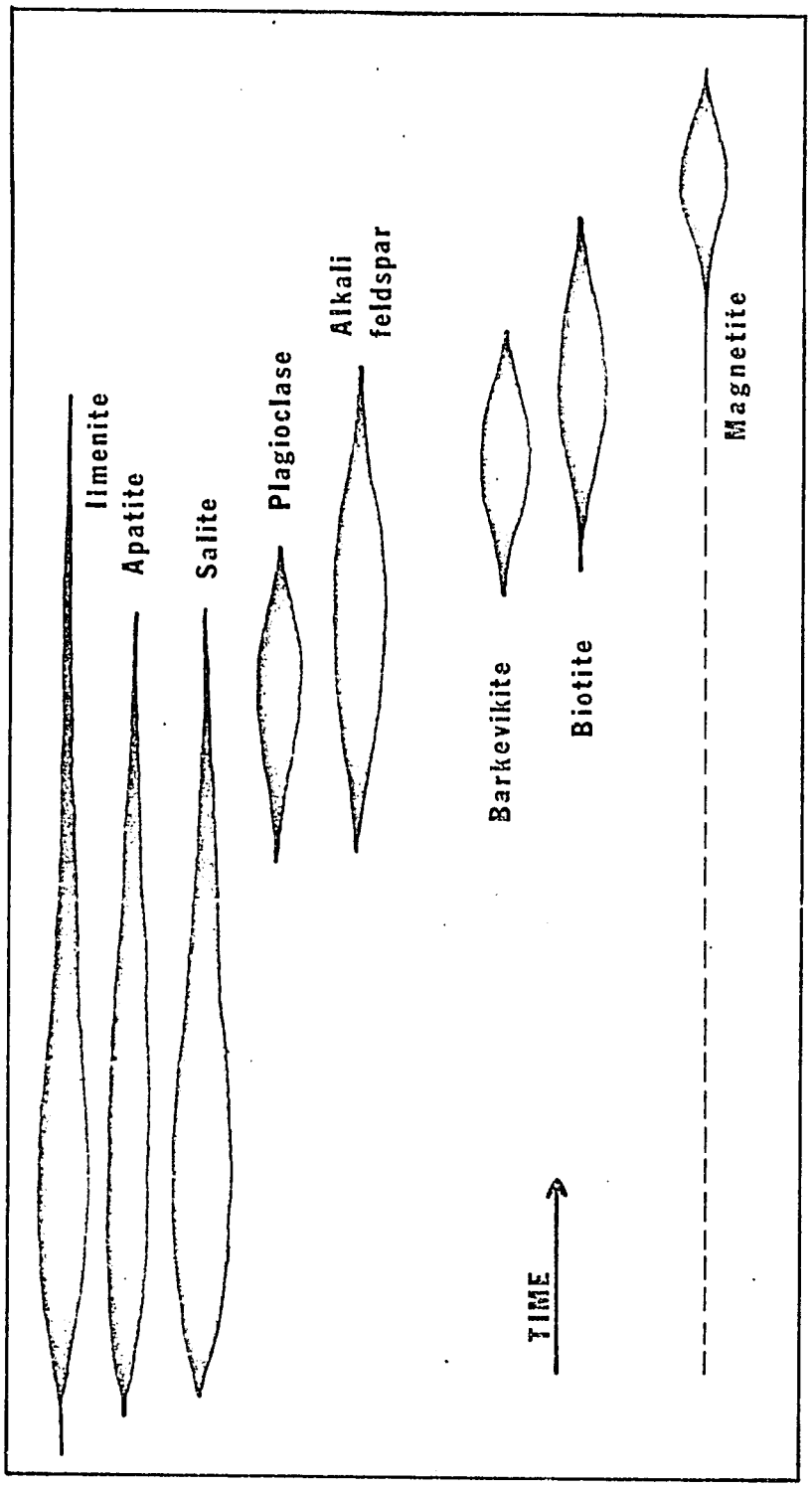

Figure 18 Schematic diagram showing the crystallization history of syenite II.

Intrusion model of syenites I and II

Any intrusion model proposed for syenites I and II must explain:

A) the distribution patterns of the minerals in the two intrusives,

B) the cumulus-like textures observed in the central part of syenite I, and the southern part of syenite II,

C) the difference in chemistry between the two intrusives, and

D) the primary horizontal lineations, and vertical foliation in syenite I.

The well ordered concentric mineralogical zoning in syenite I, suggests that some process of crystal fractionation was operative during the crystallization of the body.

Bhattacharji (1966) has suggested a process of flowage differentiation whereby the early crystallizing phases migrated to the center of the conduit up which the magma was travelling. This process could give rise to the observed geometry of syenite I. However, this process requires that some of the phases crystallize prior to emplacement. There is no evidence in support of this hypothesis.

Philpotts (1968) has suggested an interesting model to explain the distribution of rock types in Mt. Johnson, Quebec. Mt. Johnson is a vertical plug which has a younger olivine

essexite core, grading laterally to an older pulaskite margin. Throughout the intrusive there is a well developed primary foliation. In the olivine essexite there is also well developed primary layering parallel to the foliation.

According to Philpotts, the magma was intruded into relatively cold rocks. The resulting high horizontal temperature gradients would initiate vertical convection; the hot magma rising in the center, and the relatively cooler magma sinking along the walls of the pipe.

During crystallization, Philpotts postulated that the magma may have separated into two immiscible liquids, one of olivine essexite composition and the other of pulaskite composition. The latter having a lower density would accumulate at the top of the magma reservoir. This would be accompanied by the development of separate convection cells in each liquid.

Eventually, crystals would begin to stick to the walls, and the magma would begin to solidify from the walls inward. Subsequent intrusion of the lower cells into the upper ones produced the observed rock distribution and age relationship.

It is suggested that a model similar to Philpotts's model was operative during the crystallization of syenites I and II.

It is suggested that syenite I was emplaced as a largely liquid magma: perhaps containing a few suspended crystals of Mg-rich salite, apatite, and ore minerals (Figure 19A). As Philpotts (1968) pointed out, heat loss from pipe-like bodies occurs mainly along the walls of the pipe, and this heat loss normally initiates vertical convection.

As previously mentioned, the temperature gradients between the intrusive and the country rocks, do not appear to have been very great. This would result in relatively slow convection cells.

In a convecting system of this type, crystallization would probably begin along the walls. It is suggested that Mg-rich salite, apatite, and minor amounts of ore minerals started crystallizing in these parts of the magma chamber (Figure 20B). It is postulated, that the early crystals did not stick to the walls of the magma chamber; but that they were carried downward by the descending cooler magma. Initialy the hotter magma rising in the center would carry these early formed crystals upward (Figure 19B). Crystallization of large amounts of Mg-rich salite, apatite, and minor amounts of ore minerals would result in a more alkalic residual liquid. As the density contrasts between the early formed crystals and the residual liquid increased, they would begin to sink at a faster rate. If the net upward force of the magma convection was not much greater than the force of gravitational settling

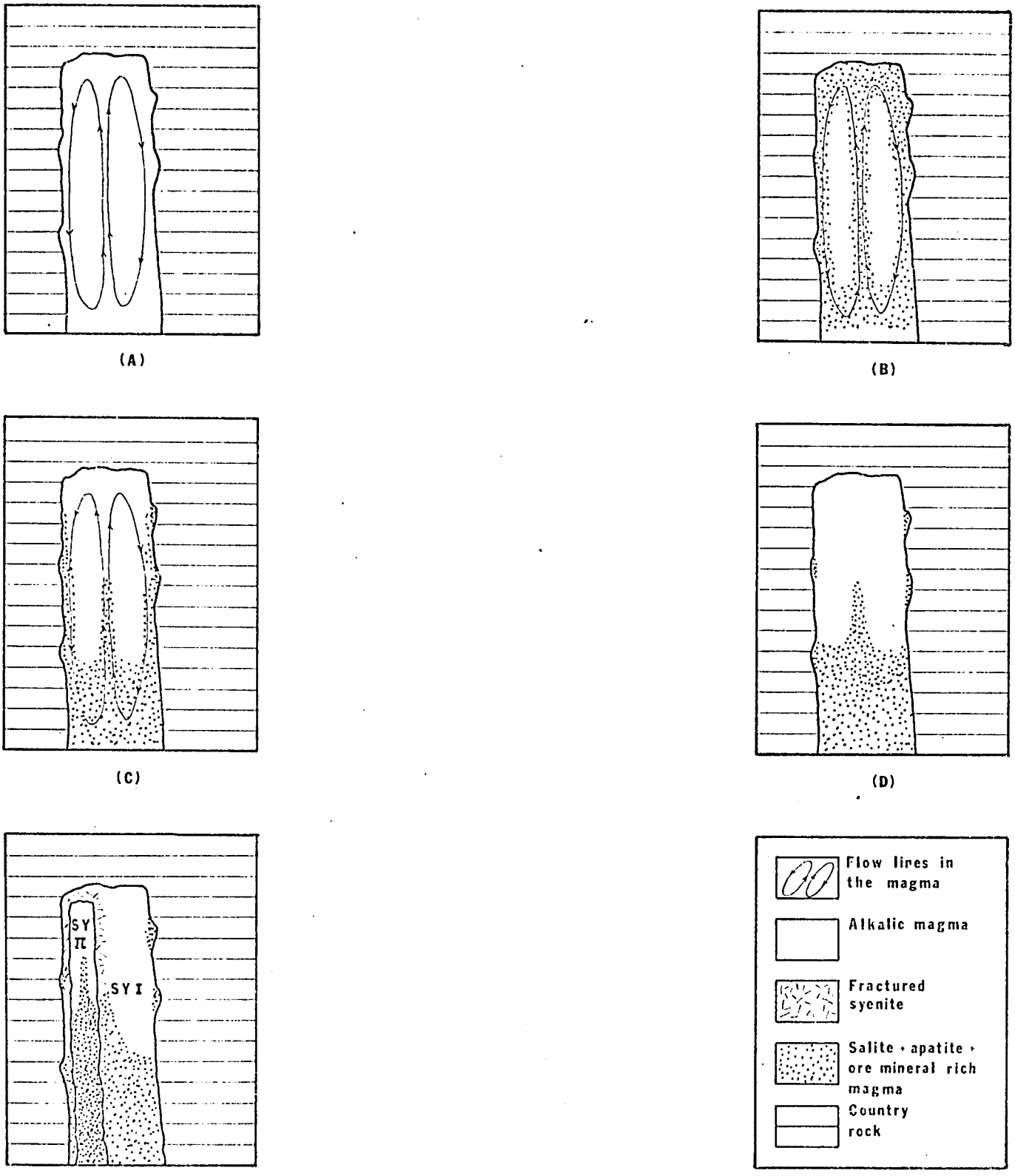

Figure 19 Schematic diagram of the intrusion model for syenites I and II.

of the crystals, the net rate of upward movement of these crystals would be small, and they would not be carried very far upward (Figure 19C).

Over a period of time, this process would result in a more alkalic magma in the upper part of the magma chamber, and a Mg-rich salite, apatite, and iron-rich magma below it(Figure 19C). Once the fractionation of the initial magma into a light upper alkalic liquid and a lower crystal mush was effected, convection is postulated as having stopped (Figure 19D). The absence of a primary foliation in most of syenite I supports this hypothesis.

Continued crystallization of apatite, and minor amounts of ore minerals, was accompanied by the crystallization of the plagioclase and potash feldspars, and the more iron-rich salite, after convection had ceased. Shortly afterwards, salite became unstable, and reacted with the residual magma to produce alkali feldspar. This was followed by the crystallization of most of the magnetite in the remaining interstitial space.

Nepheline probably started to crystallize after sufficient alkali feldspar had crystallize to lower the silica activity in the residual melt. Calcite crystallized from the late interstitial liquid.

In syenite I, the high concentrations of salite, apatite, and magnetite in the central part of the intrusive gradually decrease outward; and vice versa for microperthite. This suggests that the two liquids were not immiscible, and that some mixing took place between the two liquids.

This model provides a satisfactory explanation for the high concentrations of Mg-rich salite, apatite, ore minerals, and low concentrations of microperthite in the central part of syenite I. It also explains the cumulus-like textures in these rocks (Plates 4,10, and 19). Along the margins of syenite I, there are several small areas with high concentrations of salite, and apatite(see Figures 6 and 11). They may be due to the entrapment of early formed crystals in irregularities in the walls of the magma chamber (Figure 19D).

The distribution patterns of barkevikite and biotite follow closely that of salite (Figures 6, 7, and 8). This is what would be expected if most of these minerals were derived from the salite. The distribution pattern of primary calcite is difficult to interpret. It does not coincide very well with the distribution patterns of the other minerals (Figures 6,7,8,9,10,11, and 12). Perhaps it reflects the location of high concentrations of late stage interstitial liquids.

The circular pattern of horizontal primary lineations, and the two cases of primary vertical layering in syenite I

are somewhat problematical. Unfortunately, the structural features are insufficiently distinct to suggest a process by which they formed, or the dynamics of emplacement of syenite I.

At some later date, after syenite I had consolidated, the process was repeated with the injection of syenite II near the margin of syenite I (Figure 19E).

As in syenite I, this model provides a satisfactory explanation for the location of high concentrations of salite in the southern part of syenite II (Figure 6), and the textures observed in these rocks (Plate 5). It also provides an explanation for the distribution of apatite and ore minerals in syenite II (Figures 10 and 11).

The distribution pattern of microperthite in syenite II is similar to that in syenite I, in that low concentrations of microperthite occur in salite-rich rocks and vice versa. However, the patterns of these minerals do not coincide as closely as in syenite I (Figures 6 and 9).

The distribution pattern of barkevikite in syenite II follows that of salite, in the same manner as in syenite I. Biotite has two modes of occurrence: as small crystals which form small rims around salite and barkevikite in the marginal rocks of syenite II, and as large sheets along randomly oriented cracks and fissures. The irregular distribution pattern of biotite is, in part, due to the fact that these large flakes were included in the modal analyses.

Calcite is present in trace amounts only in syenite II. This may be due to loss of CO_2 from the system, or perhaps the partial pressure of CO_2 was initially low.

Syenite II is richer in iron, calcium, and poorer in silica, alkalis, and alumina than syenite I. If the two intrusives were derived from the fractional crystallization of a common parent magma, syenite II should be richer in iron, silica, and alkalis. This discrepancy may be due to the fractionation of substantial amounts of alkali feldspar in the parent magma prior to the emplacement of syenite II.

Parent magma of syenites I and II

The pronounced textural, mineralogical, and chemical similarities between syenites I and II suggest that they were derived from a common parent magma. Unfortunately, there is little evidence to indicate the nature of the parent magma. There is no direct evidence to suggest that syenites I and II were derived from a granitic magma by assimilation of calcareous rocks, but the calc silicate inclusions in syenite I represent possible evidence in support of this hypothesis. It is not known if these rocks were formed, during the regional metamorphism, prior to the emplacement of syenite I, or if they are the result of assimilation of calcareous rocks by syenite I.

Origin of nepheline in the country rocks

Nepheline was observed in only one locality in the country rocks (Figure 3). Keeping in mind that the Gracefield pluton is an easterly plunging pipe-like body, the nepheline-bearing gneiss is close to, and above the underground extension of the Gracefield pluton. This suggests that the nepheline may be metasomatic, and formed as a result of introduction of alumina and alkalis from syenites I and II. Payne (1968) observed the same phenomena in the country rocks along the upper border of the Blue Mountain nepheline syenite, and has suggested a similar origin for the nepheline.

CHAPTER VII

CONCLUSIONS

From field observations, petrographic, chemical, and mineralogical studies of syenites I and II, several conclusions can be drawn. They are outlined below:

A) The Gracefield pluton is composed of two distinct intrusives which are syenitic in composition. They both appear to have pipe-like forms, which dip eastwardly. Syenite II is the younger, and has intrusive relationships with syenite I.

B) Both syenites I and II appear to have intruded late in the Grenville metamorphic and tectonic history.

C) If the oxygen fugacity was close to that of the QFM buffer throughout the crystallization of syenite I, then the fugacity of water was between 302-1950 bars. The silica activity in the melt appears to have been low during crystallization of syenite I. Homogenized feldspar (now exsolution microperthite) equilibrated with nepheline at 730°C. The temperature at the time of intrusion was probably somewhat higher. Syenite I appears to have been emplaced at appreciable depths in the crust. In syenite II the oxygen and water fugacities, and temperatures of intrusion were probably similar to those in syenite I.

D) The crystallization histories of syenites I and II are very similar. Crystallization appears to have begun with the crystallization of Mg-rich salite, apatite, and minor amounts of ore minerals. Continued crystallization of minor amounts of ore minerals, and apatite was later accompanied by the crystallization of the feldspars, and more iron-rich salite. Due to decreasing temperatures and/or increasing volatile content in the magma, the salite became unstable and reacted with the melt to form barkevikite and biotite, while plagioclase reacted with the melt to form alkali feldspar. This was followed by the crystallization of magnetite in the remaining interstitial space. In syenite I, nepheline began to crystallize near the margins of the body after silica activity had been lowered to a sufficient degree through precipitation of alkali feldspar. Calcite crystallized from the late stage liquids in syenite I. In syenite II, biotite crystallized from late stage liquids on planes that possibly represent shrinkage cracks.

E) The distribution patterns of the minerals in syenites I and II, are due to the operation of convection cells during their crystallization histories.

REFERENCES

Aoki, K. 1970. Petrology of kaersutite bearing ultramafic and mafic inclusions in Iki Island, Japan. Contrib. Mineral. Petrol., vol. 25 pp 270-283.

Aubert de la Rue, 1953. Kensington area, Gatineau and Labelle Counties. Dept. of Mines, Quebec, Geol. Rept. 50.

Aubert de la Rue, 1956. Trente-et-un-milles Lake Area. Quebec Dept. of Mines, Geol. Rept. 67.

Bhattacharji, S. 1966. Mechanics of flow differentiation. Science, vol. 145, pp 150-153.

Bourne, J. 1970 Geology of the Cayamant Lake area. Quebec Dept. of Natural Resources, Preliminary Report no. 598.

Bowen, N.L. 1919. Crystallization differentiation in igneous magmas. Journal of Geology, vol. 27, pp 393-430.

Buddington, A.F. and Lindsley, D.H. 1964. Iron- titanium oxide minerals and synthetic equivalents. Journal of Petrology, vol. 5, pp 310-357.

Carmichael, I.S.E., Nicholls, J. and Smith, A.L. 1970. Silica activity in igneous rocks. American Mineralogist, vol. 55, pp 246-253.

Carmichael, I.S.E., Turner, F.J., and Verhoogen J. 1974. Igneous Petrology. McGraw - Hill Book Company, New York.

Deer, W.A., Howie, R.A., and Zussman, J. 1963. Rock-forming Minerals. vol. 2: Chain silicates. Longmans, Green and Co. Ltd. London.

Deer, W.A., Howie, R.A., and Zussman, J. 1966. Introduction to Rock-forming Minerals. Longmans, Green and Co. Ltd. London.

Doig, R., and Barton, J.R. 1968. Ages of carbonatites and other alkaline rocks in Quebec. Canadian Journal of Earth Sciences, vol. 5, pp 1401-1408.

Ells, R.W. 1907. Report on the geology and natural resourses of the area included in the northwest quarter sheet number 122 of the Ontario and Quebec series, comprising portions of the counties of Pontiac, Carleton and Renfrew. Geol. Surv. Canada, separate Report 977.

Essene, E.J., and Fyfe, W.S. 1967. Omphacite in Californian metamorphic rocks. Contrib. Mineral. Petrol., vol. 15, pp 1-23.

Gunn, B.M. 1972. The fractionation effectsof kaersutite in basaltic magmas. Canadian Mineralogist, vol. 11, pp 840-850.

Hamilton, D.L., and MacKenzie, W.S. 1965. Phase equilibrium studies in the system $NaAlSiO_4$(nepheline) - $KAlSiO_4$(kalsilite) - SiO_2- H_2O. Mineral. Mag., vol. 34, pp 214-231.

Jen, L.S. 1973. The determination of iron(II) in silicate rocks and minerals. Analytica Chimica Acta, vol. 66, pp 315-318.

Legris, P. 1972. The petrology of a syenite pluton near Renfrew, Ontario. Unpublished BSc Thesis, University of Ottawa, Ottawa, Canada.

Luth, W.C., Fenn, P.M., and Martin, R.F. 1970. Thermodynamic excess functions, relative activities, and solvus relations for synthetic alkali feldspars. Geological Society of America, Abstracts with Programs, pp 611-612.

Millhollen, G.L. 1971. Melting of nepheline syenite with H_2O and $H_2O + CO_2$, and the effect of dilution of the aqueous phase on the beginning of melting. American Journal of Science, vol. 270, no.3, pp 244-254.

Morse, S.A. 1968. Syenites. Carnegie Institution Year Book, vol. 67, pp 112-113.

Nash, W.P., and Wilkinson, J.F.G. 1970. Shonkin Sag laccolith, Montana. Mafic minerals and estimates of temperature oxygen fugacity, and silica activity. Contrib. Mineral. and Petrol., vol. 25, pp 241-265.

Osborn, E.F. 1959. Role of oxygen pressure in the crystallization and differentiation of basaltic magma, American Journal of Science, vol. 257, pp 609-647.

Payne, J.G. 1968. Geology and geochemistry of the Blue Mountain nepheline syenite. Canadian Journal of Earth Sciences, vol. 5, pp 259-272.

Perchuk, L.L., and Ryabchikov, I.D. 1968. Mineral equilibria in the system nepheline-alkali feldspar-plagioclase, and their petrological significance. Journal of Petrology, vol. 9, pp 123-167.

Philpotts, A.R. 1968. Igneous structures and mechanism of emplacement of Mount Johnson, a Monteregian intrusion, Quebec. Canadian Journal of Earth Sciences, vol. 5, pp 1131-1137.

Powell, M., and Powell, R. 1975. A Nepheline-alkali feldspar geothermometer. Extended Abstracts, International Conference on Geothermometry and Geobarometry, Pennsylvania State University.

Robie, R.A., and Waldbaum, D.R. 1968. Thermodynamic properties of minerals and related substances at 298.15°K (25.0°C) and one atmosphere (1.013 bars) pressure and at higher temperatures. U.S. Geological Survey, Bull. 1259.

Rucklidge, J., and Gasparrini, E.L. 1969. Electron microprobe data reduction(EMPADR VII). Dept. Geology, University of Toronto.

Rutherford, M.J. 1973. The phase relations of aluminous iron biotites in the system $KAlSi_3O_8$-$KAlSiO_4$-Al_2O_3-Fe-O-H. Journal of Petrology, vol. 14, pp 159-180.

Savelli, C. 1967. The problem of rock assimilation by Somma and Vesuvius lavas. Contrib. Mineral. Petrol. vol. 16, pp 328-353.

Spry, A. 1969. Metamorphic Textures. Pergamon Press, New York.

Vennor, H.G. 1878. Progress report of explorations and surveys made during the years 1875 and 1876 in the counties of Renfrew, Pontiac and Ottawa. Geol. Surv. Canada, Report of progress for 1876-1877, pp 244-320.

Watkinson, D.H., and Wyllie, P.J. 1971. Experimental Study of the composition join $NaAlSiO_4$-$CaCO_3$-H_2O and the genesis of alkalic rock-carbonatite complexes. Journal of petrology, vol. 12, pp 357-378.

Winkler, H.G.F. 1974. Petrogenesis of Metamorphic Rocks. Third Edition, Springer - Verlag, New York.

Wones, R.D., and Eugster, H.P. 1965. Stability of biotite: experiment, theory, and application. American Mineralogist, vol. 50, pp 1228-1272.

Wones, R.D. 1972. Stability of biotite: a reply. American Mineralogist, vol. 57, pp 316-317.

Wynne-Edwards, H.R., Gregory, A.F., Hay, P.W., Giovanella, C.A., Reinhardt, E.W. 1966. Mont Laurier and Kempt Lake map areas, Quebec. Geol. Surv. Can., Paper 66-32.

Plate 1

Partial assimilation of gneissic band, and segregation of felsic and mafic minerals. Gn = gneiss, AF = alkali feldspar, P = diopsidic pyroxene, S = Syenite.

Plane Light Magnification 0.8X

Specimen MD-170


S
S
S
AF
AF
P
P
Gn

Plate 2

Mortar textures in paragneiss.

Mp = microperthite, Pl = plagioclase, Bio = biotite.

Crossed Polars. Magnification 17X

Specimen MD-13A


Bio
Mp & Pl
Mp
Pl
Mp
Mp
Mp

Plate 3

Mortar textures in syenite I.

Emp = exsolution microperthite, B = barkevikite,

Om = ore minerals, Sp = sphene, Bio = biotite,

AF = alkali feldspar.

Crossed Polars. Magnification 17X

Specimen MD-43

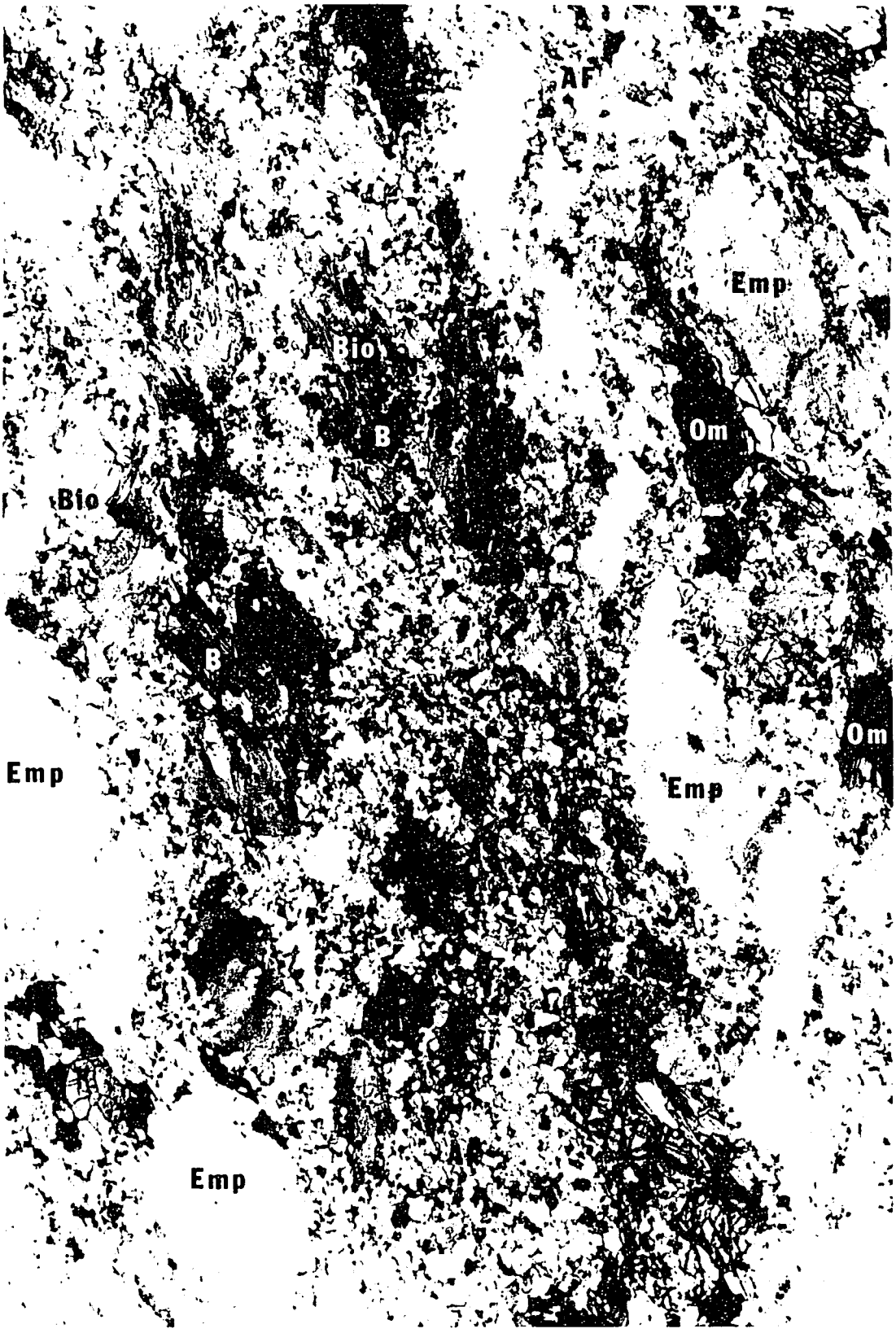
AF
Emp
Bio
B
Om
Bio
B
Om
Emp
Emp
Emp

Plate 4

Cumulus-like salite in syenite I with intercumulus barkevikite, exsolution microperthite, ore minerals, Sa = salite, Emp = exsolution microperthite, Ap = apatite, Om = ore minerals, B = barkevikite.

Plane Light Magnification 17X

Specimen MD-90


Om
Sa
Om
Emp
Ap
B
B
Ap
B
Bio
Om
Sa
Emp

Plate 5

Cumulus-like salite in syenite II with intercumulus barkevikite, ore minerals, and microperthite.

Sa = salite, B = barkevikite, Emp = exsolution microperthite, Bio = biotite, Ap = apatite, Om = ore minerals.

Plane Light Magnification 17X

Specimen MD-73

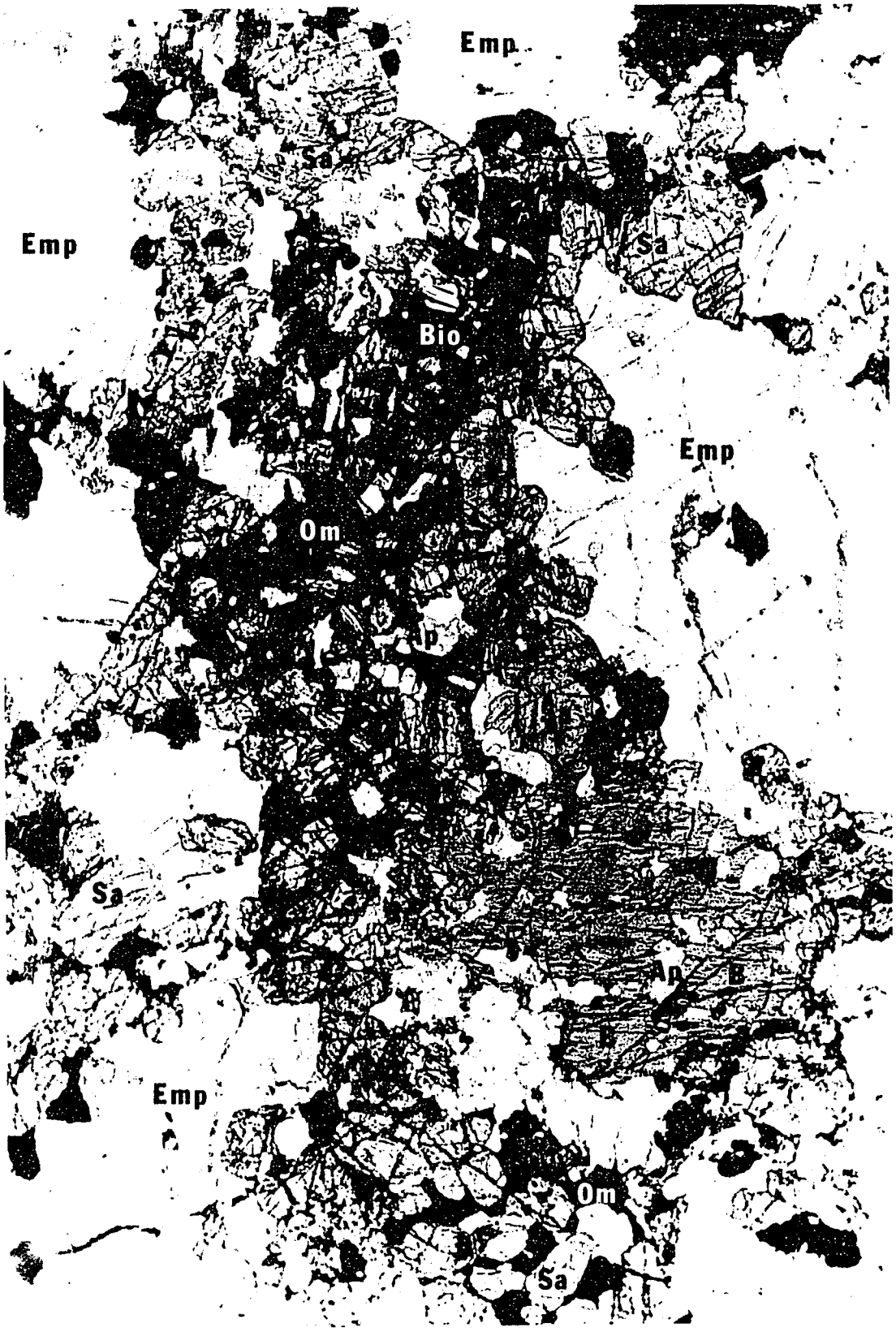
Emp
Emp
Sa
Sa
Bio
Emp
Om
Jp
Sa
Ap
B
Emp
Om
Sa

Plate 6

Interstitial salite. Sa = salite,

B = barkevikite, Bio = biotite,

Rmp = replacement micropertite.

Crossed Polars Magnification 17X

Specimen MD-98


Rmp
Rmp
Sa
Bio
Rmp
Sa

Plate 7

Salite grain surrounded by a partial rim of barkevikite and biotite. Sa = salite, B = barkevikite, Bio = biotite, Rmp = replacement microperthite, Om = ore minerals.

Plane Light Magnification 50X

Specimen MD-22

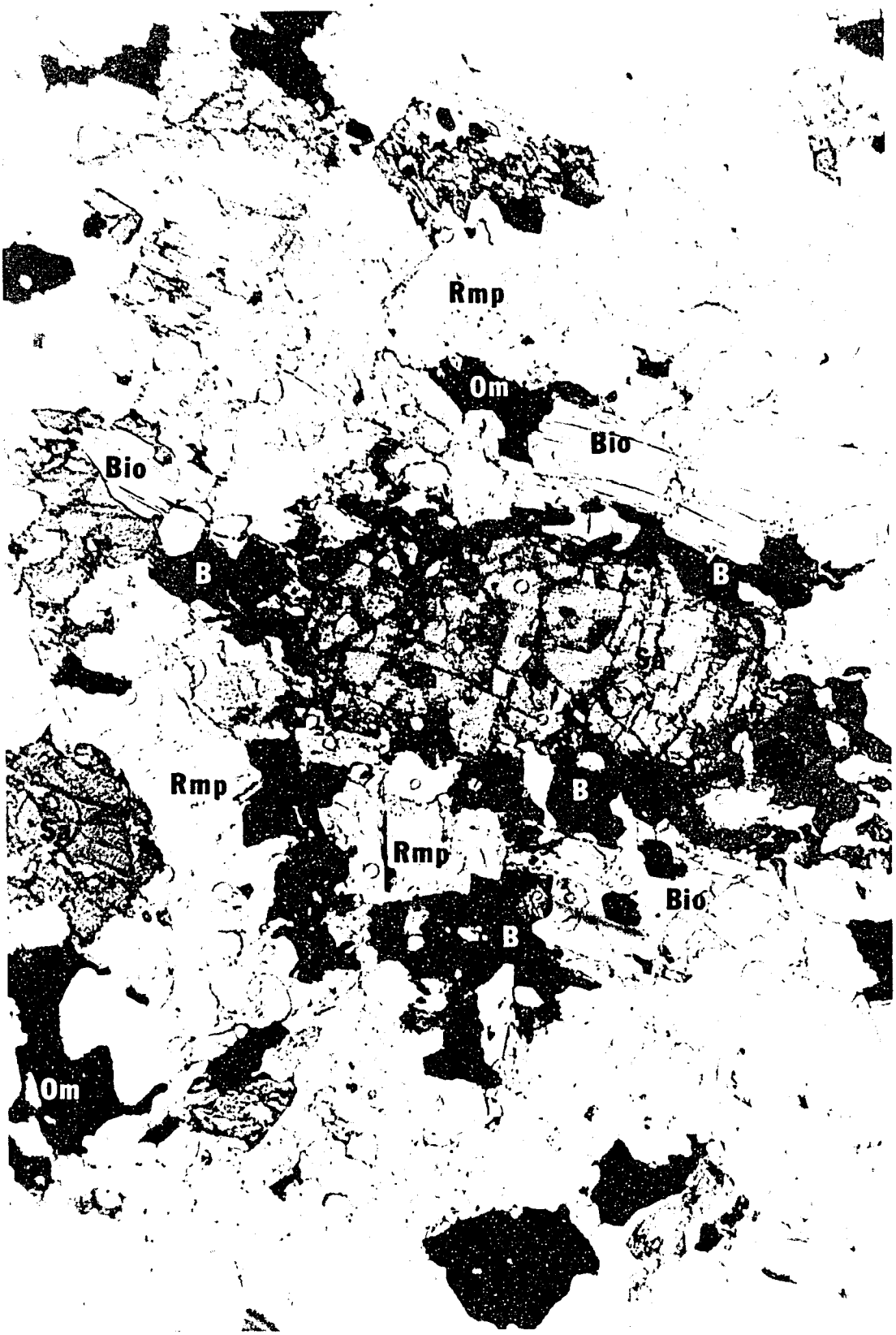
Rmp
Om
Bio
Bio
B
B
Rmp
B
Rmp
Bio
B
Om

Plate 8

Exsolution of magnetite lamellae along cleavage planes in salite. Sa = salite, Rmp = remplacement microperthite, Ap = apatite, Om = ore minerals, El = exsolution lamellae of magnetite.

Plane Light Magnification 105X

Specimen MD-99


Om
El
Rmp
Ap
Sa
Rmp

Plate 9

Salite grains partially altered to uralite.

Sa = salite, Rmp = replacement microperthite,

Ap = apatite, Bio = biotite,

Om = ore minerals.

Plane Light Magnification 50X

Specimen MD-86


Rmp
Sa
Ap
Ap
Sa
Om
Ap
Om
Rmp
Rmp
Sa
Bio

Plate 10

Small biotite crystals occurring as small patches in salite, and as partial rims around salite, ore mineral and barkevikite grains. Sa = salite, B = barkevikite, Om = ore mineral, Bio = biotite, Ap = apatite, Emp = exsolution microperthite.

Plane Light Magnification 17X

Specimen MD-113

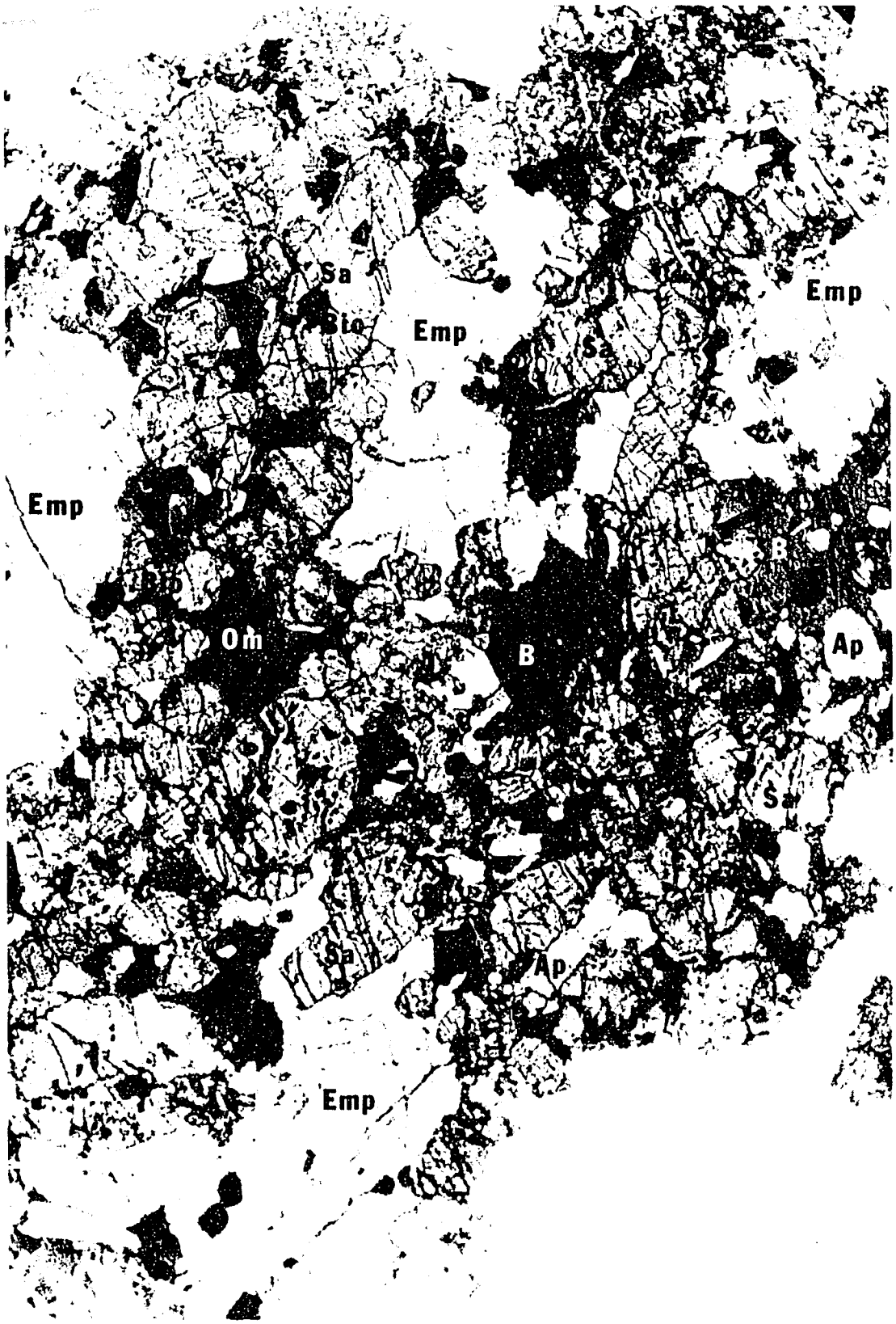
Sa
Bio
Emp
Emp
Sa
Emp
Emp
B
Om
B
Ap
Sa
Sa
Ap
Emp

Plate 11

Interstitial biotite crystals. Bio = biotite, Rmp = replacement microperthite, Sa = salite, B = barkevikite.

Crossed Polars Magnification 17X

Specimen MD-103

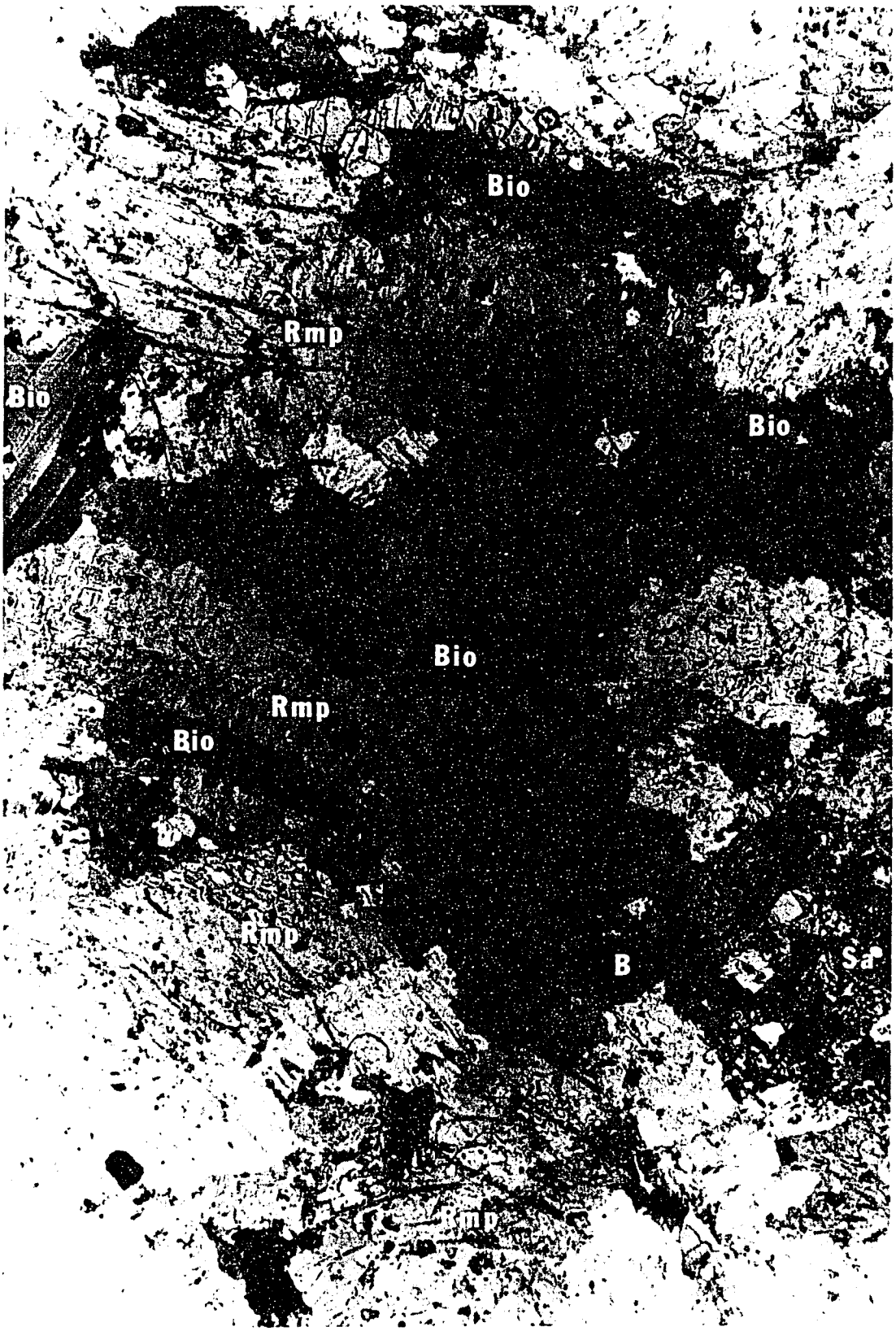
Bio
Rmp
Bio
Bio
Bio
Rmp
Bio
Rmp
B
Sa
mp

Plate 12

Large biotite crystals. Note that all the biotite in this plate has the same optical orientation. Bio = biotite, Sa = salite, Om = ore minerals, Ap = apatite, Rmp = replacement microperthite.

Plane Light Magnification 17X

Specimen MD-30


Bio
Rmp
Bio
Om
Rmp
Om
Ap
Ap
Bio
Rmp
Rmp
Bio

Plate 13

Specimen showing very large biotite flakes.

Plane Light Magnification 1.2X

Specimen MD-170

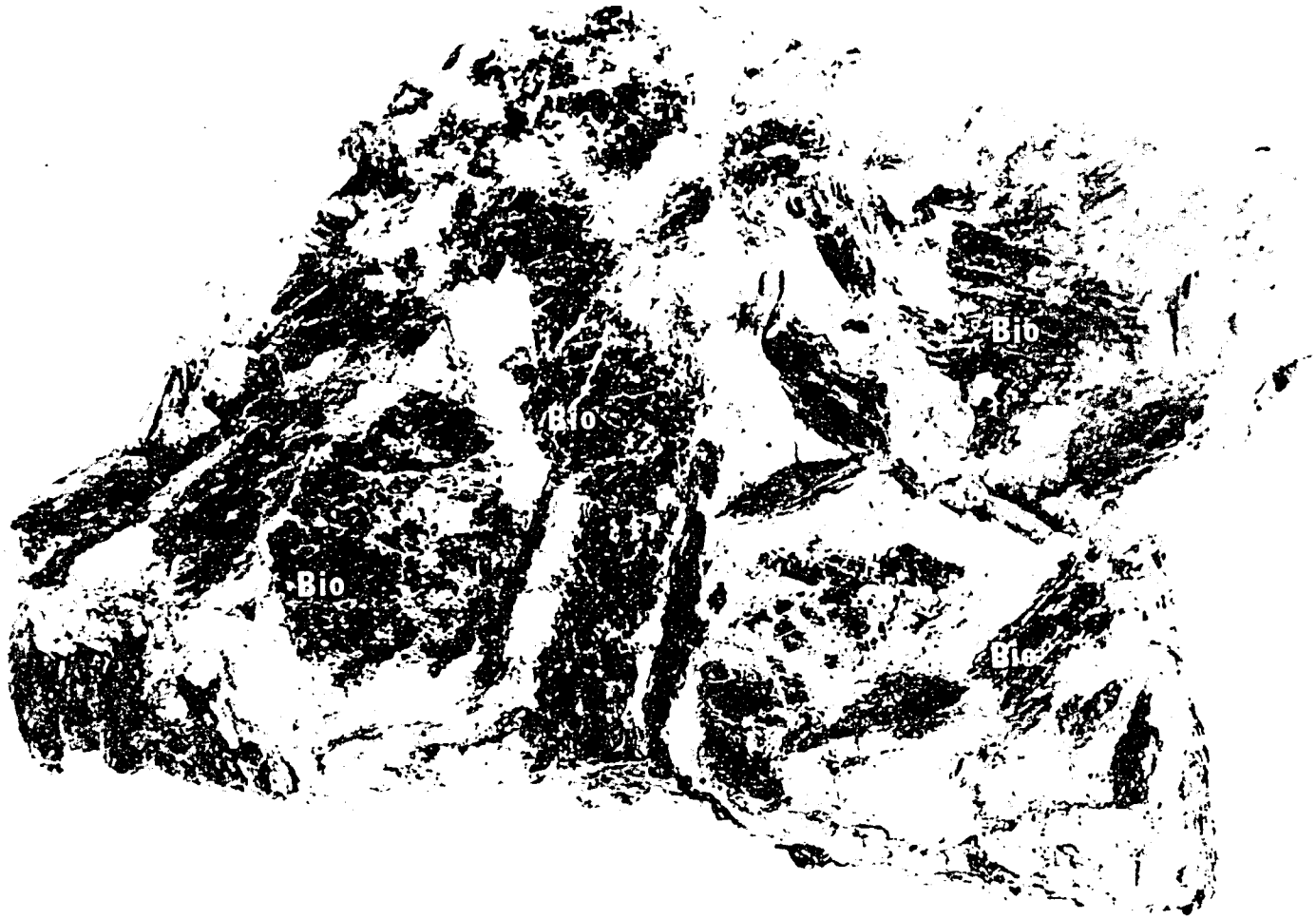
Bio
Bio
Bio
Bio
Bio

Plate 14

Replacement microperthite crystal. The lighter colored patches labelled Pl are relict plagioclase. Emp = exsolution microperthite.

Crossed Polars Magnification 50X

Specimen MD-89

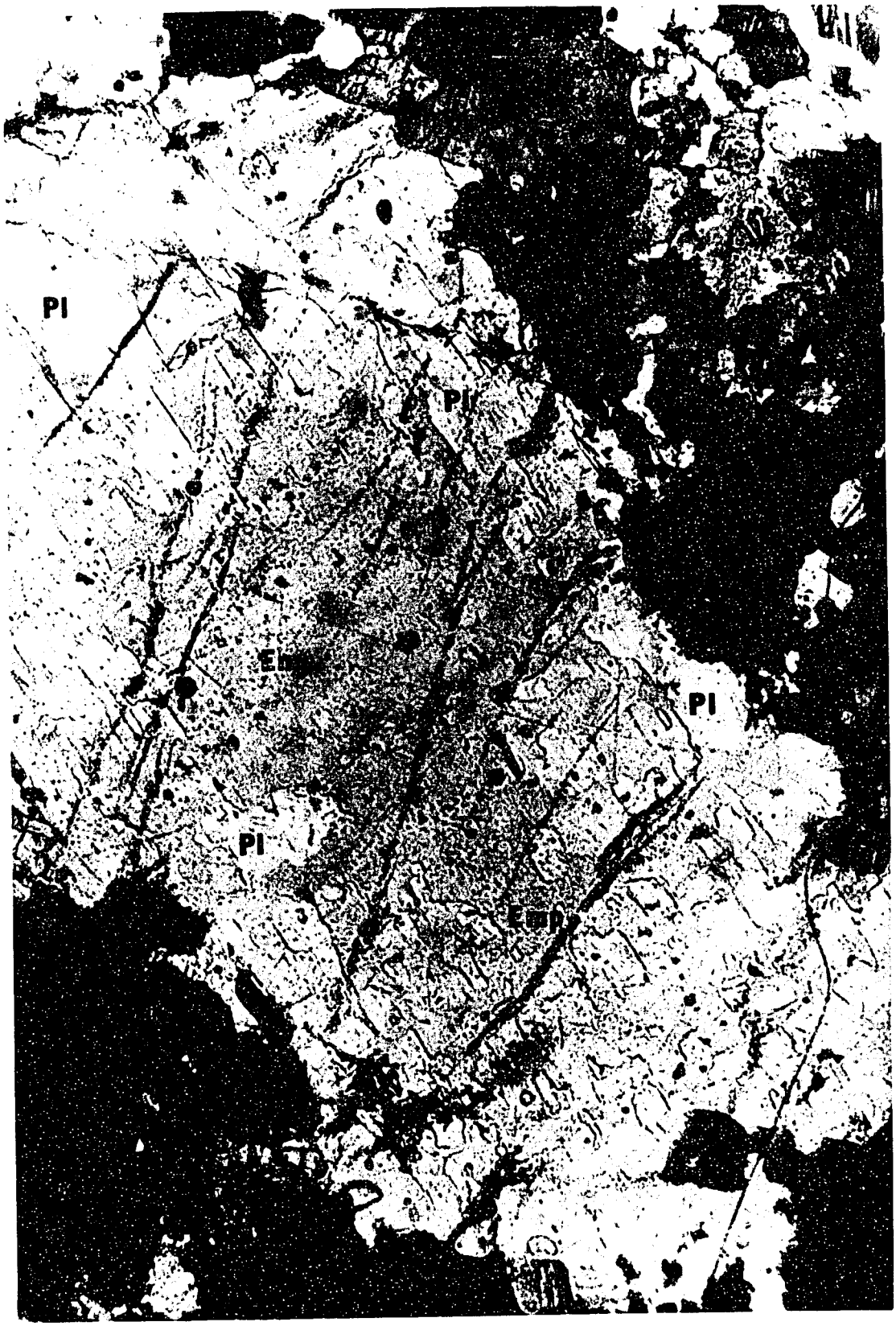
Pl
Pl
Pl
Pl

Plate 15

Badly corroded and deeply embayed plagioclase crystal. Pl = plagioclase, Emp = exsolution microperthite.

Crossed Polars Magnification 50X

Specimen MD-72

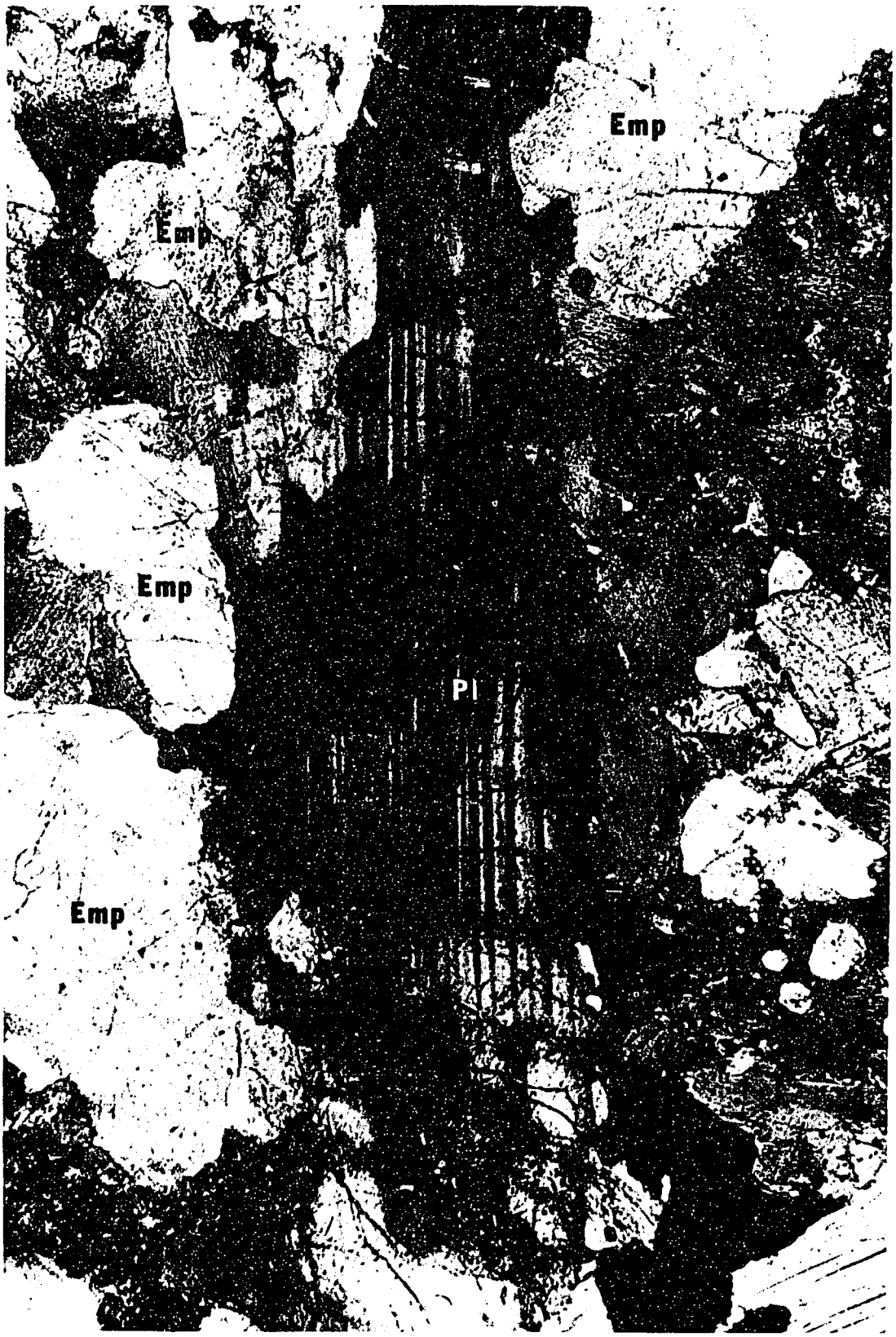
Emp
Emp
Emp
Emp
Emp
Pl

Plate 16

Plagioclase crystal which is partially replaced by exsolution microperthite. Pl = plagioclase, Emp = exsolution microperthite.

Crossed Polars Magnification 50X

Specimen MD-64


Emp
Emp
Pl
Pl
Emp

Plate 17

Plagioclase crystal which is partially replaced by exsolution microperthite. Pl = plagioclase, Emp = exsolution microperthite, Rmp = replacement microperthite, Om = ore minerals.

Crossed Polars Magnification 50X

Specimen MD-66


Rmp
Pl
Pl
Emp
Emp
Om

Plate 18

Replacement microperthite crystal. Plagioclase relicts are present as irregular blebs, strings, and rods scattered throughout the crystal. Pl = plagioclase, Sa = salite, Om = ore minerals. Darker colored areas in the crystal are alkali feldspar.

Crossed Polars Magnification 50X

Specimen MD-96


Sa
Om
Pl
Pl
Pl
Pl

Plate 19

Intercumulus microperthite crystals enclosing several salite and apatite crystals. Emp = exsolution microperthite, Sa = salite, B = barkevikite, Ap = apatite, Om = ore minerals.

Plane Light Magnification 17X

Specimen MD-113

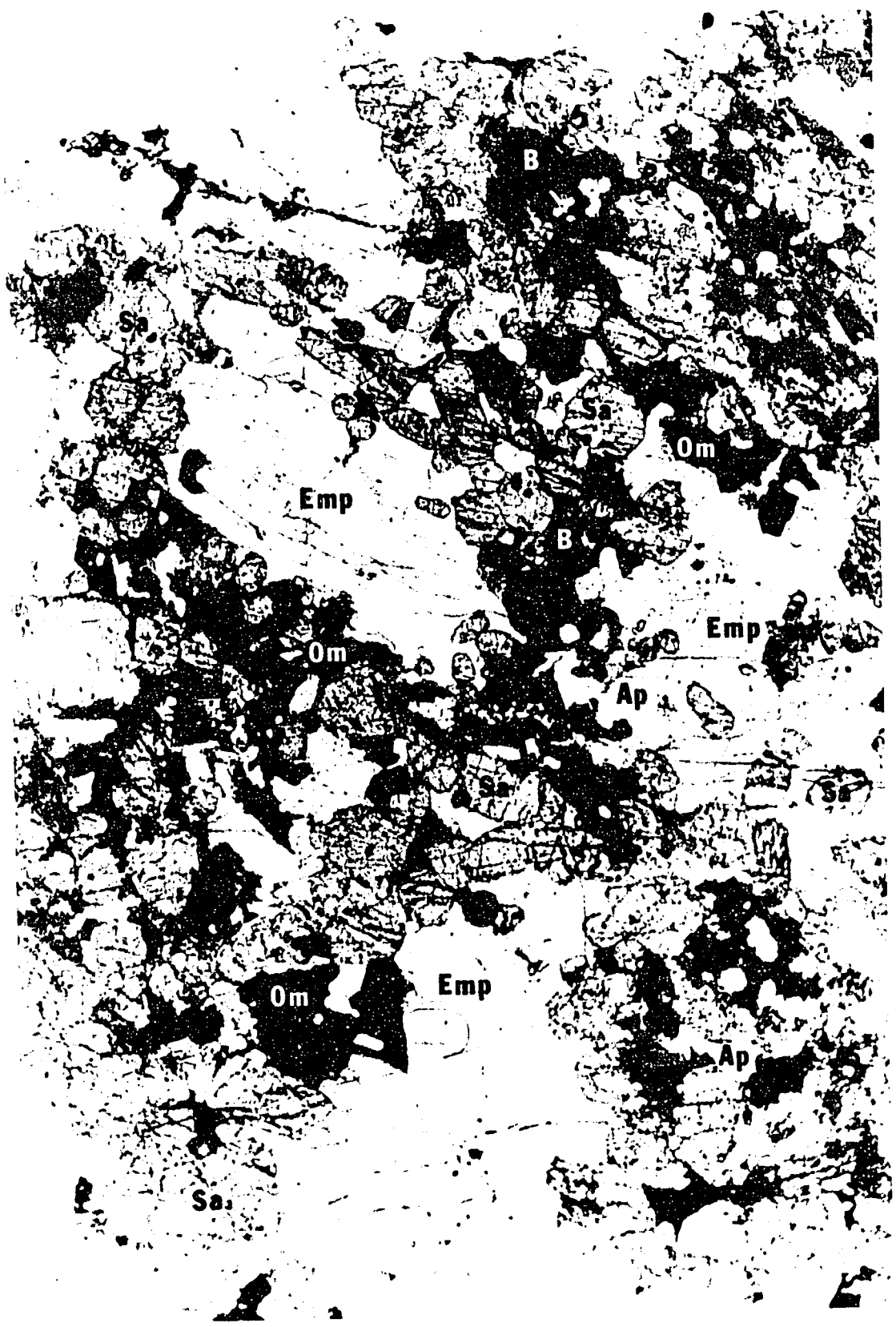
B
Sa
Sa
Om
Emp
B
Om
Emp
Ap
Sa
Sa
Om
Emp
Ap
Sa

Plate 20

Plate showing the two modes of occurrence of nepheline (A) as interstitial crystals, and (B) as inclusions in exsolution microperthite. Ne = nepheline, Emp = exsolution microperthite, Bio = biotite, Om = ore minerals.

Crossed Polars Magnification 17X

Specimen MD-84


Emp
Ne
Emp
Ne
Emp
Ne
Ne
Om
Ne
Ne
Ne

Plate 21

Large exsolution microperthite crystal containing several grains of nepheline. Nepheline grains are surrounded by a small rim of albite. Emp = exsolution microperthite, Ne = nepheline, Ab = albite, Bio = biotite

Crossed Polars Magnification 105X

Specimen MD-87


Ab
Emp
Emp
Ab
Bio
Ab
Emp